© 2016. Published by The Company of Biologists Ltd | Development (2016) 143, 398-410 doi:10.1242/dev.130849

STEM CELLS AND REGENERATION

TECHNIQUES AND RESOURCES ARTICLE

WNT/β-catenin signaling mediates human neural crest induction via a pre-neural border intermediate

Alan W. Leung[1,2], Barbara Murdoch[3], Ahmed F. Salem[4], Maneeshi S. Prasad[4], Gustavo A. Gomez[4] and Martín I. García-Castro[1,4,*]

ABSTRACT

Neural crest (NC) cells arise early in vertebrate development, migrate extensively and contribute to a diverse array of ectodermal and mesenchymal derivatives. Previous models of NC formation suggested derivation from neuralized ectoderm, via meso-ectodermal, or neural-non-neural ectoderm interactions. Recent studies using bird and amphibian embryos suggest an earlier origin of NC, independent of neural and mesodermal tissues. Here, we set out to generate a model in which to decipher signaling and tissue interactions involved in human NC induction. Our novel human embryonic stem cell (ESC)-based model yields high proportions of multipotent NC cells (expressing SOX10, PAX7 and TFAP2A) in 5 days. We demonstrate a crucial role for WNT/β-catenin signaling in launching NC development, while blocking placodal and surface ectoderm fates. We provide evidence of the delicate temporal effects of BMP and FGF signaling, and find that NC development is separable from neural and/or mesodermal contributions. We further substantiate the notion of a neural-independent origin of NC through PAX6 expression and knockdown studies. Finally, we identify a novel pre-neural border state characterized by early WNT/β-catenin signaling targets that displays distinct responses to BMP and FGF signaling from the traditional neural border genes. In summary, our work provides a fast and efficient protocol for human NC differentiation under signaling constraints similar to those identified *in vivo* in model organisms, and strengthens a framework for neural crest ontogeny that is separable from neural and mesodermal fates.

KEY WORDS: β-Catenin signaling, Embryonic stem cells, Human, Neural border, Neural crest

INTRODUCTION

Neural crest (NC) is a transient multi-potent cell population that emerges between the forming neural plate and the non-neural/surface ectoderm. The 'new head' model (Gans and Northcutt, 1983) proposed that the NC was an evolutionary advancement that distinguished vertebrates from other chordates, and linked the derivatives of NC and cranial placodes to the predatory life style of vertebrates. Interestingly, NC and cranial placodes were further proposed to derive from single precursors (Baker and Bronner-Fraser, 1997; Gans and Northcutt, 1983), and phylogenetic studies suggested that their lineages diverted after the neural-epidermal segregation in the early ectoderm (Groves and LaBonne, 2014; Patthey and Gunhaga, 2014; Schlosser, 2008). In avian embryos, neural induction is thought to initiate slightly before or during gastrulation (Streit et al., 2000; Wilson et al., 2000, 2001), and specification and lineage assays identified the lateral epiblast at early gastrula stages as poised to form NC independently of neural fate (Basch et al., 2006; Patthey et al., 2009). In pre-gastrula amphibian embryos, evidence for establishment of a neural boundary via planar signaling was reported (Savage and Phillips, 1989; Zhang and Jacobson, 1993). A recent study in amphibians proposes a shared genetic regulatory network of blastula pluripotent cells with developing NC cells at the neural border (Buitrago-Delgado et al., 2015). These studies in avian and amphibian embryos hint at an early fate specification for NC. Recent human embryo studies have validated several markers of pre-migratory NC cells (Betters et al., 2010) but, similar to rodents and other mammals, no information has been published regarding earlier stages of specification or induction of NC. Interspecific differences in NC development have been postulated (Barriga et al., 2015); it remains unclear when mammalian NC cells are specified during development and if their induction involves mesoderm and neural tissues. There is an urgent need to develop and optimize models for mammalian NC development to study these aspects.

Embryonic stem cells (ESCs) or induced pluripotent stem cells (iPSCs), derived from mouse, primate and human blastocysts, have been extensively employed for studies of developmental processes that otherwise are difficult to carry out *in vivo* (Evans, 2011; Pera and Trounson, 2004; Rodda et al., 2002; Sasai, 2013; Spagnoli and Hemmati-Brivanlou, 2006). The current methods for generating human NC tissue, however, often involve dense self-organizing cell conglomerates (embryoid bodies, neural rosettes, or confluent cultures) that produce autocrine signaling. They also include steps and components that have precluded the elucidation of the specific signaling pathways and tissue contributions required for the early stages of human NC formation.

Here, we set out to develop a suitable model in which to study the contributions of specific signaling pathways and early embryonic tissues during human NC formation. We establish a culture system that generates human NC cells validated with markers demonstrated in human embryos (Betters et al., 2010). Furthermore, our protocol demonstrates cost effectiveness, high efficiency and unprecedented speed, and dispenses with the use of serum replacement, heregulin, activin antagonists, and the pre-differentiation (ESC expansion) period employed by previous protocols (Chambers et al., 2013; Fukuta et al., 2014; Menendez et al., 2011; Mica et al., 2013; Umeda et al., 2015). Our study demonstrates a key role for canonical WNT signaling in human NC formation, confirming contributions from bone morphogenetic protein (BMP) and fibroblast growth factor (FGF) pathways and supports an independent origin of NC

[1]Kline Biology Tower, Department of Molecular, Cellular and Developmental Biology, Yale University, 266 Whitney Avenue, New Haven, CT 06511, USA. [2]Yale Stem Cell Center, 10 Amistad Street, New Haven, CT 06519, USA. [3]Department of Biology, Eastern Connecticut State University, 83 Windham St., Willimantic, CT 06226, USA. [4]203 School of Medicine Research Building, School of Medicine, University of California Riverside, Riverside, CA 92521, USA.

*Author for correspondence (martin.garcia-castro@ucr.edu)

Received 21 September 2015; Accepted 21 December 2015

Development (2016) 143, 398-410 doi:10.1242/dev.130849

from PAX6$^+$ neural progenitors. Furthermore, our study suggests a distinct cellular origin of human NC cells through a novel early intermediate that precedes and is differentially regulated from the neural border cells.

RESULTS

WNT elicits rapid differentiation of human ESCs into neural crest-like cells

To enable a clearer analysis of the signaling pathways and possible tissue contributions involved in early human NC development, we employed low-density cultures of dissociated human ESCs (hESCs) in defined serum free-media under WNT activation (Fig. 1A). We chose to study the effect of WNT signaling because it has been shown to be instrumental in NC induction in both human and animal models (Garcia-Castro et al., 2002; Menendez et al., 2011; Mica et al., 2013). We plated 20,000 hESCs/cm^2 in DMEM/F12 medium, plus B27 supplement and bovine serum albumin, and employed CHIR 99021 (CHIR, a GSK3 inhibitor) to activate WNT signaling. CHIR-treated WA01 hESCs, Y6 iPSCs and RIV9 iPSCs displayed robust expression of the characteristic NC markers SOX10, PAX7 and TFAP2A by day 5 (Fig. 1B-D; Fig. S1; data not shown). In the absence of CHIR, human ESCs did not generate SOX10- or PAX7-expressing cells (Fig. 1B). The differentiating cells expanded by 9.3±1.5 times under CHIR treatment and resulted in 63.1±9.6% SOX10$^+$, 78.6±7.9% PAX7$^+$ and 84.4±7.6% TFAP2A$^+$ cells (Fig. 1C). The vast majority (~95%) of the SOX10$^+$ cells co-expressed PAX7 and TFAP2A (Fig. 1D). The remaining SOX10$^+$ cells co-expressed either TFAP2A (~5%) or PAX7 (<0.5%). Transcriptional analysis of a panel of NC markers (*PAX3*, *PAX7*, *TFAP2A*, *SNAI2*, *ZIC1*, *MSX1*,

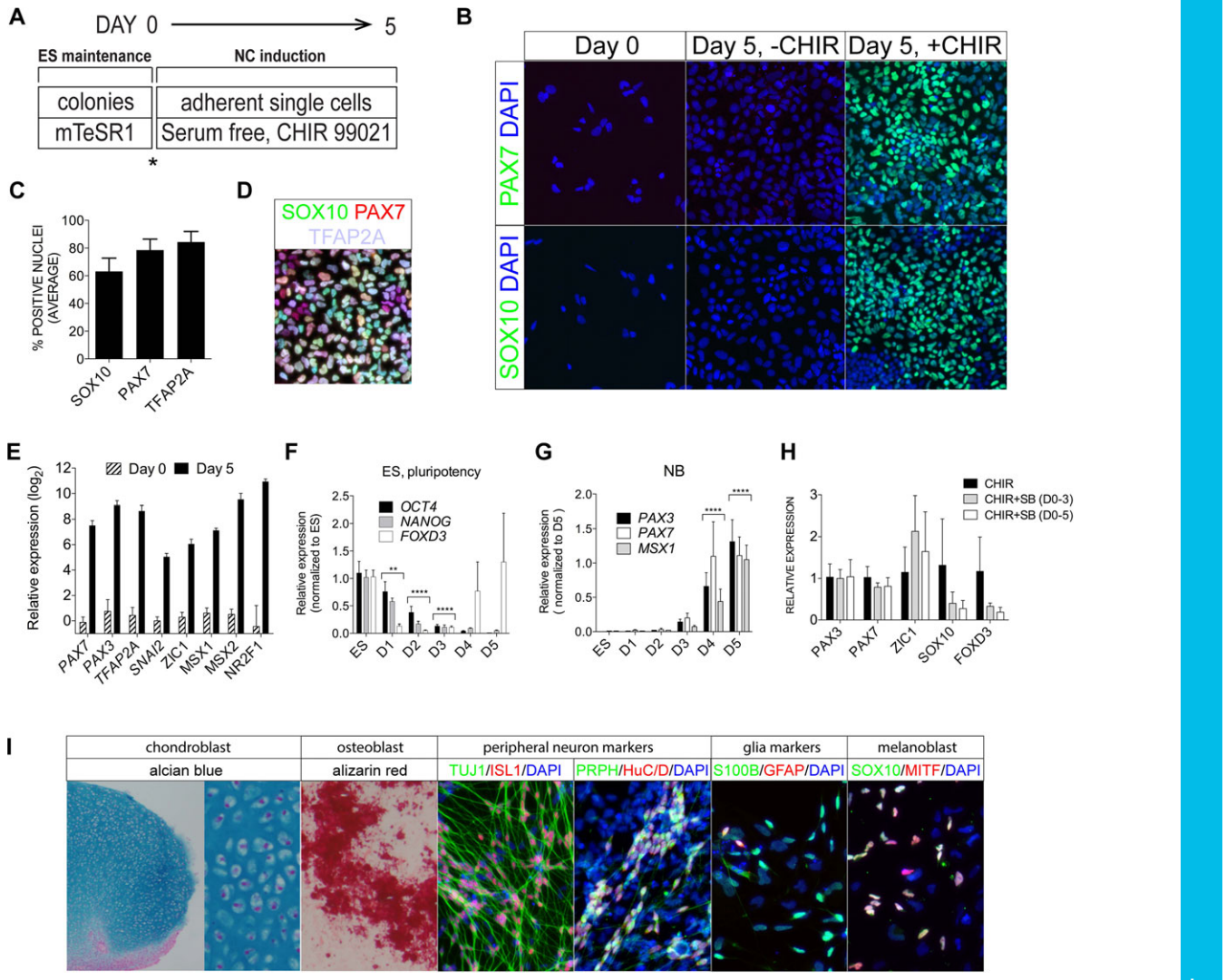

Fig. 1. WNT-mediated induction of multipotent NC-like cells from hESCs. (A) Scheme for maintaining and differentiating hESCs into NC cells. Asterisk indicates the enzymatic passage and subsequent plating in differentiation medium to start differentiation. (B) SOX10 and PAX7 immunostaining (green) and DAPI nuclear staining (blue) in dissociated ESCs at day 0, day 5 control (D5–CHIR) and CHIR-treated (D5+CHIR) cultures. (C) SOX10$^+$, PAX7$^+$ and TFAP2A$^+$ nuclear counts in D5+CHIR cultures. (D) Triple-immunostaining for SOX10 (green), PAX7 (red) and TFAP2A (violet) in D5+CHIR cultures. (E) RT-qPCR analyses of NC markers at day 5 with expression levels normalized to ESC controls (day 0). (F,G) Daily time course analyses from day 0 (D0) to day 5 (D5) for ESC/pluripotency (F) and neural border (NB) (G) markers. $^{**}P \leq 0.01$, $^{****}P \leq 0.0001$. (H) RT-qPCR analyses of NC transcripts in +CHIR cultures treated with SB 431542 (SB) for 0, 3 or 5 days. (I) Differentiation of NC derivatives. Alcian Blue and Alizarin Red staining in day 30 cultures differentiated under chondrogenic and osteogenic conditions, respectively. Markers associated with peripheral sensory neurons (PRPH, HuC/D, TUJ1 and ISL1), glia (GFAP and S100β) and melanoblasts (MITF, SOX10; Mica et al., 2013) were detected after culturing +CHIR hNC with SU-5402, CHIR99021 and DAPT for an additional week (13 days total). Error bars represent s.e.m. Data were pooled from three or more independent experiments.

Development (2016) 143, 398-410 doi:10.1242/dev.130849

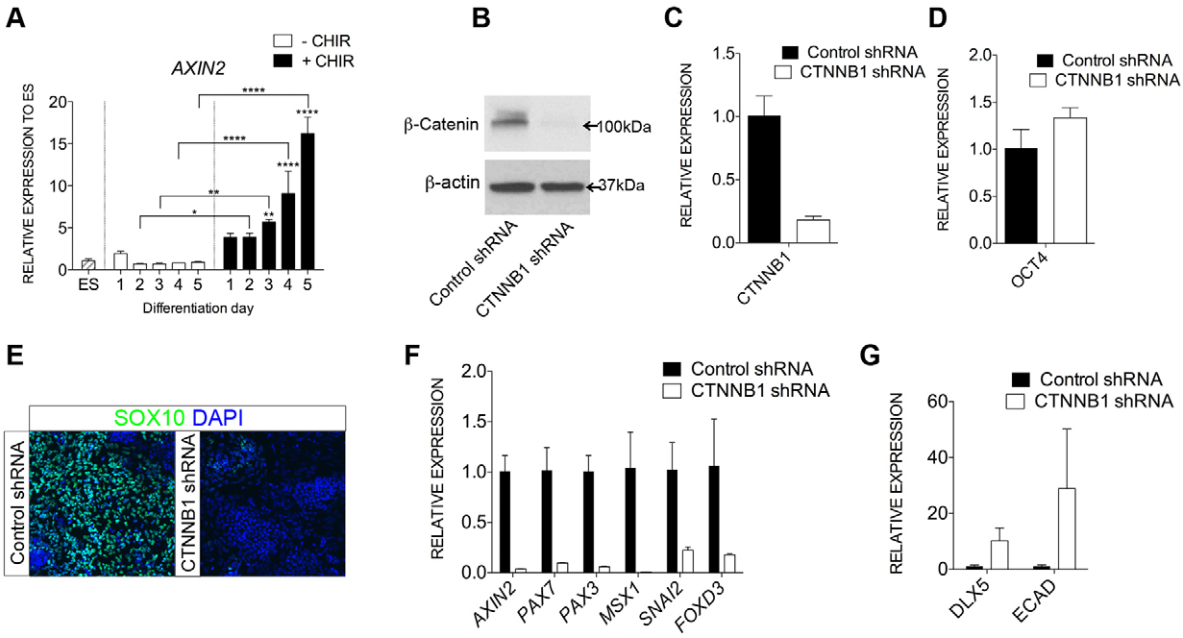

Fig. 2. WNT/β-catenin signaling is required for human NC induction. (A) Time course of expression (RT-qPCR) for *AXIN2* in hESCs treated with (+) or without (–) CHIR. *$P \leq 0.05$, **$P \leq 0.01$, ****$P \leq 0.0001$. At least three independent experiments performed for panel A data; error bars represent s.e.m. (B) Western blot of β-catenin and β-actin expression in control (luciferase) and *CTNNB1* shRNA-treated ESCs (ladder sizes indicated). (C,D) RT-qPCR analysis of *CTNNB1* and *OCT4* expression in control and *CTNNB1* shRNA-treated ESCs. (E) Effect of control or *CTNNB1* shRNA on NC induction (D5+CHIR cultures) analyzed by SOX10 immunostaining. (F,G) RT-qPCR analyses of NC (F) and non-neural ectodermal (G) genes in D5+CHIR cultures treated with control or *CTNNB1* shRNA. Results from one representative experiment (out of two independent experiments) presented for *CTNNB1* knockdown; error bars represent s.d. in C,D,F,G.

MSX2, *NR2F1*) revealed that expression levels of these markers were increased by 30- to 2000-fold (Fig. 1E). CHIR substitution by Wnt3a in our culture conditions also led to robust NC induction (as revealed by SOX10-PAX7 immunostaining, and PCR of NC markers; data not shown).

NC-like cells have been reported to arise spontaneously from cultures plated at high densities (Leung et al., 2013). Indeed, $CHIR^-$ control cultures seeded at 50,000-100,000 cells/cm^2 generated $PAX7^+$ and $SOX10^+$ cells (Fig. S2A,B). Importantly, inhibition of WNT signaling through DKK1 or the tankyrase inhibitor XAV 939 (Fig. S2C,D) repressed the induction of NC markers, suggesting a role of paracrine WNT signaling in NC induction.

Upon CHIR treatment, expression of the hESC markers *OCT4* (*POU5F1* – Human Gene Nomenclature Database), *NANOG* and *FOXD3* was greatly reduced by day 3 of differentiation (Fig. 1F). *FOXD3*, which is also expressed by NC cells, increased dramatically from day 4 onwards. In accordance with this, expression of the early NC genes (or so-called neural border genes) *PAX7*, *PAX3*, *MSX1* and *TFAP2A* (Basch et al., 2006; de Croze et al., 2011; Sato et al., 2005; Tribulo et al., 2003) was increased at day 3 by 7- to 50-fold (normalized to undifferentiated ESCs) and more robustly by day 4 (Fig. 1G; Fig. 3D). Their expression continued to rise or was maintained at day 5, when the majority of the $SOX10^+$ cells arose (Fig. 1B; Fig. 6A), indicating the acquisition of a definitive NC fate.

Activin/TGFβ antagonism does not promote human neural crest induction

Previous NC induction protocols frequently employed activin/TGFβ antagonism using the type I Activin/TGFβ receptor inhibitor SB 431542 (Chambers et al., 2013; Menendez et al., 2011; Mica et al., 2013). Transient (3 days) and continuous (5 days) treatment with SB 431542 in our differentiating cultures had either no promoting effect on early NC gene induction (*PAX3* and *PAX7*) or severely repressed the expression of mature markers (*SOX10* and *FOXD3*) (Fig. 1H), suggesting that short-term or prolonged activin/TGFβ antagonism had a negative effect on human NC induction.

Terminal differentiation of WNT-induced human neural crest derivatives

To assess further the human NC-like cells generated by WNT induction, we tested their capacity to contribute to terminal derivatives associated with NC. CHIR-treated cells subjected to terminal differentiation (see Materials and Methods) form ectomenchymal and non-ectomenchymal derivatives (Fig. 1I), including chondrocytes, osteoblasts, peripheral neurons [HuC/D^+ (ELAVL3/4), $TUJ1^+$ (TUBB3) $PRPH^+$, $ISL1^+$], glial precursors ($S100\beta^+$ $GFAP^{+/-}$) and melanoblasts ($MITF^+$ $SOX10^+$). Similar results were obtained with WNT3A-treated cells (Fig. S3), demonstrating the multipotency of our WNT-induced NC cells.

β-Catenin signaling mediates human neural crest induction

To determine the mechanism of action of CHIR in our NC induction model, we measured transcription of *AXIN2*, a canonical WNT target gene (Lustig et al., 2002). We found that it progressively increased day by day under CHIR treatment, whereas its transcription remained unchanged in non-treated cultures (Fig. 2A). We therefore performed knockdown of *CTNNB1* (β-catenin), a key mediator of the transcriptional response of canonical WNT signaling. Transduction of *CTNNB1* short hairpin (sh)RNA dramatically repressed protein expression and transcription (>80%) of the *CTNNB1* gene, compared with control (luciferase) shRNA transduction (Fig. 2B, C; Table S2). Although repression of *CTNNB1* did not repress expression of *OCT4* at the ESC stage (Fig. 2D), induction of

Development (2016) 143, 398-410 doi:10.1242/dev.130849

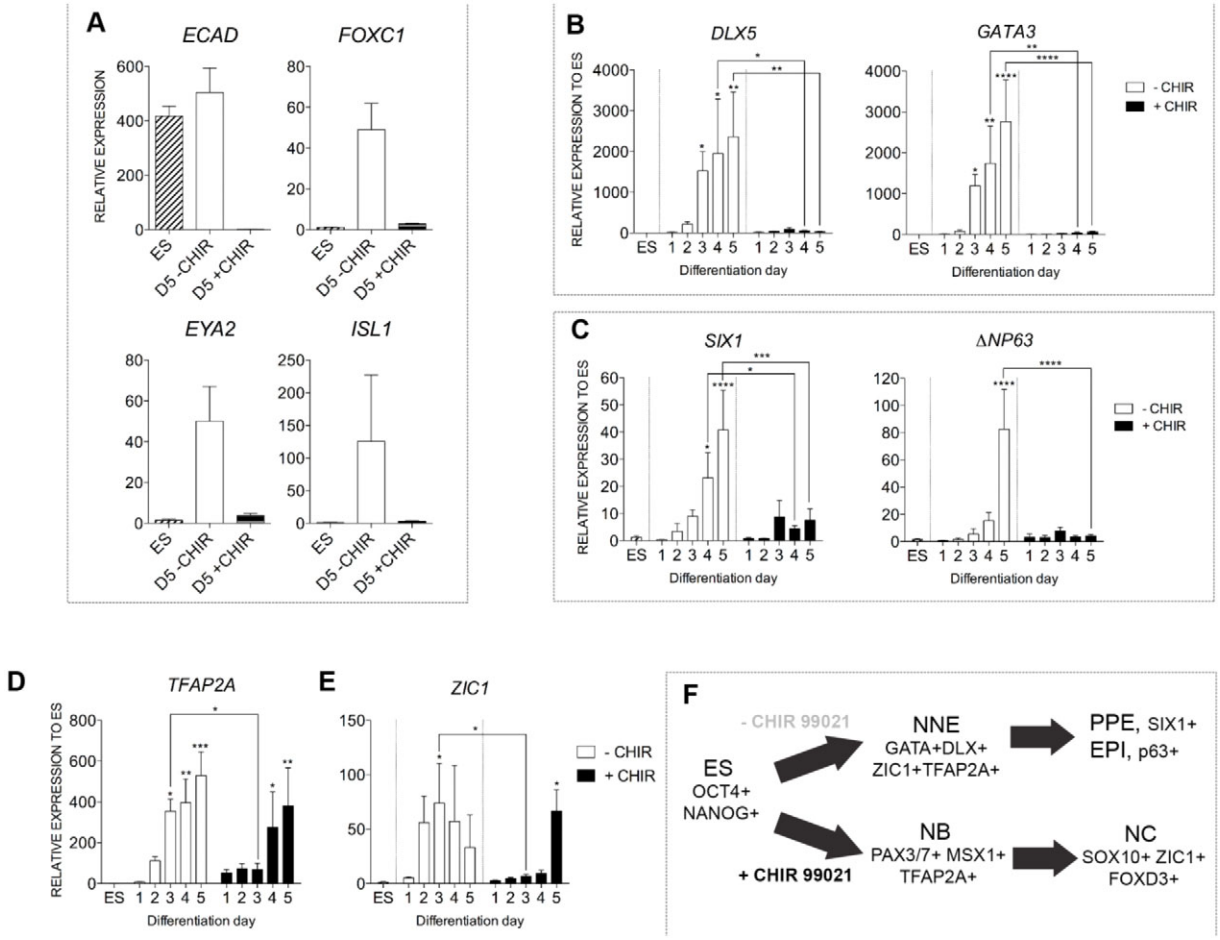

Fig. 3. WNT restricts non-neural ectoderm fate in differentiating hESCs. (A) Quantitative gene expression analysis of placodal and/or surface ectoderm associated transcripts (*ECAD*, *FOXC1*, *EYA2*, *ISL1*) in ESCs (ES), D5+CHIR or D5−CHIR cultures. (B-E) Quantitative gene expression analysis in control ESCs, −CHIR and +CHIR cultures from day 1 to day 5, for competent non-neural ectoderm (*DLX5* and *GATA3*; B), preplacodal ectoderm (*SIX1*; C), epidermal progenitor (*ΔNP63*; C) and prospective neural border (*TFAP2A* and *ZIC1*; D,E) genes. (F) Model depicting the stage-wise *in vitro* differentiation of placodal/epidermal ectoderm and NC cells. EPI, epidermal progenitors; NNE, non-neural ectoderm; PPE, preplacodal ectoderm. All panels normalized to ESCs except for *ECAD* in panel A, which is normalized to day 5 CHIR-treated cultures. Error bars represent s.e.m. Data were pooled from three or more independent experiments. *$P\leq0.05$, **$P\leq0.01$, ***$P\leq0.001$, ****$P\leq0.0001$.

SOX10^{+} cells (Fig. 2E) and transcription of key NC markers including *PAX7*, *PAX3*, *MSX1*, *SNAI2* and *FOXD3* was dramatically reduced (Fig. 2F). Reducing *CTNNB1* expression partially rescued expression of selected non-neural ectoderm genes [*DLX5* and *ECAD* (*CDH1*), but not, for example, *GATA3*] (Fig. 2G) suggesting a requirement for restricted WNT signaling for non-neural ectoderm induction (Dincer et al., 2013; Leung et al., 2013).

Early segregation of neural crest and cranial placode fates during hESC differentiation

Given the proposed fate relationships between placodes and NC, we decided to address the possible contribution of these relationships in our system. We found that the gene encoding the epithelial cell-cell adhesion molecule E-cadherin (*CDH1*, which is also highly expressed in hESCs), and the nuclear factors *FOXC1*, *EYA2* and *ISL1* were highly induced in control day 5 cultures (Fig. 3A). Upon CHIR administration, however, these surface ectoderm and preplacodal ectoderm-associated transcripts were repressed to basal levels (Fig. 3A). In a time course assay, we observed that the early non-neural ectoderm markers *DLX5* and *GATA3* were progressively induced in control cultures, and were induced 1 to 2 days earlier than the preplacodal ectoderm marker *SIX1* and the epidermal ectoderm marker *ΔNP63* (an isoform of *TP63*), respectively, confirming the sequential induction of competence and maturation markers during human placodal ectoderm cell induction (Fig. 3B,C) (Dincer et al., 2013; Leung et al., 2013). CHIR treatment curtailed the progressive induction of early (*DLX5* and *GATA3*) and mature (*ΔNP63* and *SIX1*) non-neural ectoderm markers, suggesting that canonical WNT activation restricts non-neural ectoderm induction (Fig. 3B,C) and simultaneously promotes NC induction (Fig. 3F).

Competence factors common for both NC and cranial placodes have also been identified, including *Tfap2a* and *Zic1* (de Croze et al., 2011; Hong and Saint-Jeannet, 2007; Kwon et al., 2010; Phillips et al., 2006; Streit and Stern, 1999; Tribulo et al., 2003). Both *TFAP2A* and *ZIC1* were induced at high levels at the first few days of cranial placode (−CHIR) induction and displayed significantly higher expression levels than the NC (+CHIR)-inducing condition at differentiation day 3 (Fig. 3D,E). Under the NC (+CHIR) condition, both genes were only induced by day 4 or 5, suggesting that they were mature NC markers. Induction of these factors, therefore, was differentially regulated during human NC and cranial placode development, and supports an early segregation

Development (2016) 143, 398-410 doi:10.1242/dev.130849

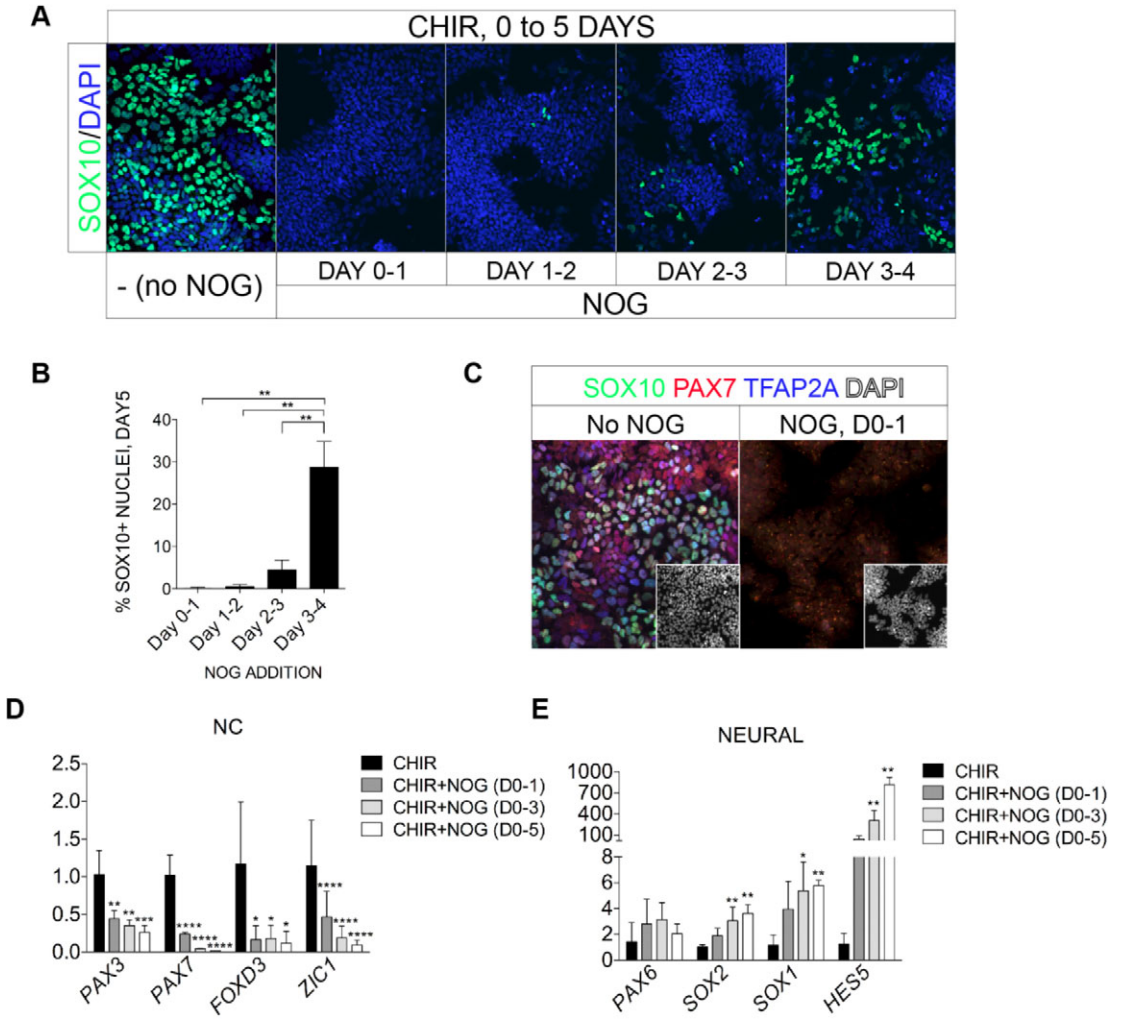

Fig. 4. BMP inhibition represses NC and promotes neural induction. (A) NC induction revealed by SOX10 immunostaining was monitored on D5+CHIR cultures exposed to the BMP inhibitor noggin (NOG, 300 ng/ml) for the indicated intervals. (B) Quantification of SOX10$^+$ cells in cultures treated with NOG as indicated in A. One-way ANOVA was carried out with Tukey's multiple comparison tests. (C) Triple immunostaining for SOX10 (green), PAX7 (red) and TFAP2A (blue) of D5+CHIR control cultures (No NOG), or with one day of NOG (D0-1) treatment. DAPI staining (white) is shown in insets. (D,E) Quantitative gene expression analysis for NC (D) and neural (E) transcripts in D5+CHIR control cultures treated with NOG for the indicated intervals. One-way ANOVA was carried out with Fisher's LSD test. Asterisks above bars indicate statistical significant difference of those treatments against CHIR controls. *P≤0.05, **P≤0.01, ***P≤0.001, ****P≤0.0001. Error bars represent s.e.m. for data pooled from three or more independent experiments.

of NC and cranial placode progenitors prior to the establishment of the neural border stage (Fig. 3F).

Human neural crest induction requires an early and balanced BMP activity

The BMP signaling pathway has also been strongly implicated in NC induction in model organisms (Stuhlmiller and Garcia-Castro, 2012a). We found that blockage of BMP signaling with the BMP inhibitor noggin at 300 ng/ml from day 0, day 1 or day 2, for 24 h, led to a dramatic inhibition of human NC induction to levels below 5% of the total cell population (Fig. 4A,B). BMP blockade from day 3 to day 4 instead only partially curtailed NC induction (28.7±6% SOX10$^+$ cells). Noggin treatment from day 0 to day 1 also eliminated PAX7$^+$ and TFAP2A$^+$ cells, as indicated by the absence of staining of day 5 cultures with SOX10, PAX7 and TFAP2A antibodies (Fig. 4C). In agreement with the antibody staining results, noggin treatments of 1 day, 3 days or 5 days duration all repressed transcription of NC markers, and 24 h of noggin treatment from day 0 to day 1 was sufficient to significantly repress NC gene transcription, indicative of an early essential role of BMP activity in NC induction (Fig. 4D). Noggin treatments correspondingly promoted transcription of neural-related genes, including *SOX1*, *HES5* and *SOX2*, in agreement with the role of BMP repression in neural induction (Fig. 4E). Neural induction appeared to require continuous BMP repression as 5 days of noggin treatment led to the highest expression level of *HES5*, a mature neuroepithelial marker (Fig. 4E).

We found that noggin treatment from day 0 to day 1 did not affect expression of the WNT target *AXIN2* in a time course experiment (measured at day 1, day 3 and day 5) suggesting that BMP signaling might have a direct role during the early phase of NC induction (data not shown). WNT has been suggested to cooperate with BMP signaling to induce neural plate border formation in avian embryos (Patthey et al., 2009). Continuous or transient treatment with BMP4 ligand (20 ng/ml) with CHIR, however, dramatically repressed induction of the early NC genes *PAX3* and *PAX7* (Fig. 5A). BMP4 ligand also repressed expression of neural-related genes (*PAX6* and *SOX2*; Fig. 5B) but promoted the transcription of genes indicative of non-neural ectoderm (e.g. *GATA3*, *DLX5* and *ECAD*; Fig. 5C).

Development (2016) 143, 398-410 doi:10.1242/dev.130849

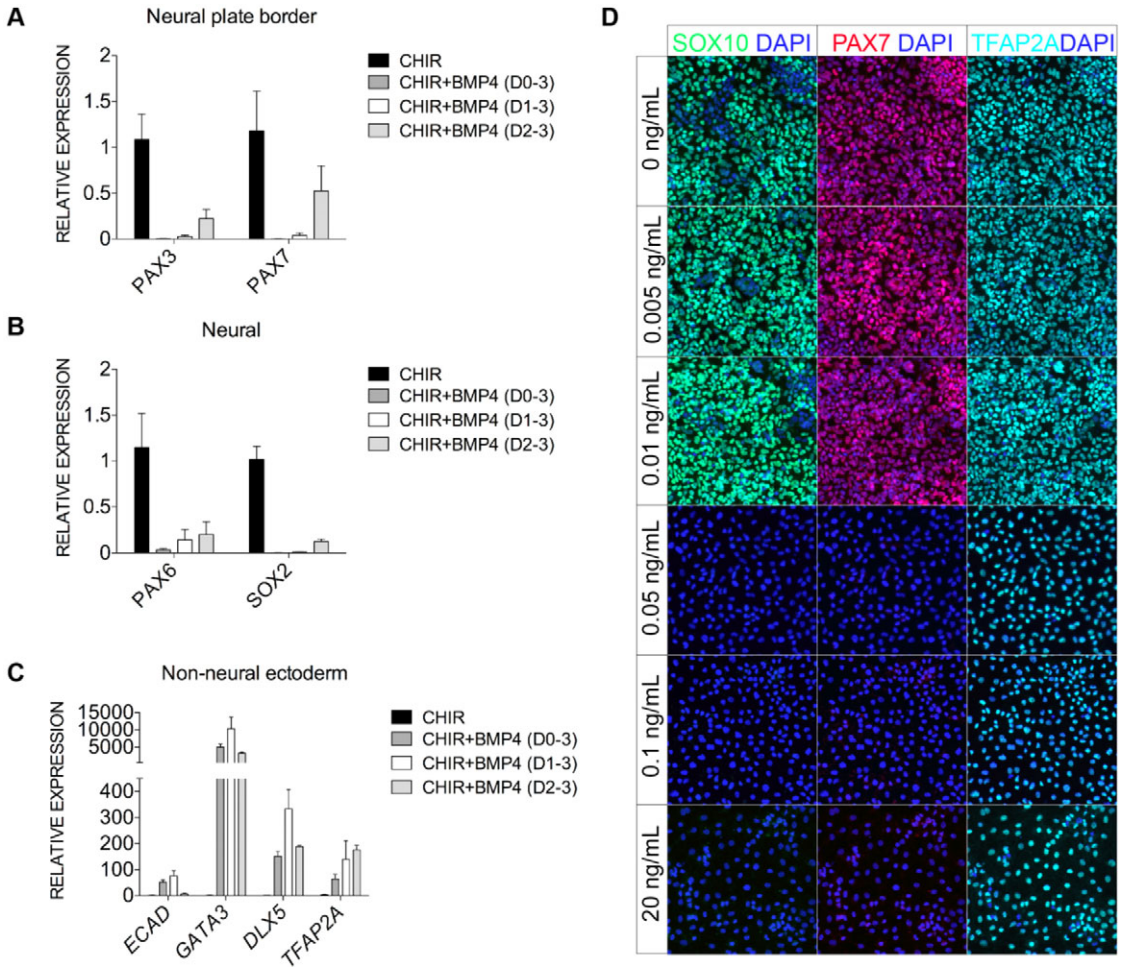

Fig. 5. Exogenous BMP4 suppresses NC but de-represses the non-neural ectoderm. (A-C) Quantitative gene expression analyses for neural border (*PAX3* and *PAX7*; A), neural-related (*PAX6* and *SOX2*; B) and non-neural ectoderm (*ECAD*, *GATA3*, *DLX5* and *TFAP2A*; C) genes in day 3 +CHIR cultures treated with BMP4 (20 ng/ml) for the indicated intervals (expression normalized to +CHIR). Error bars represent s.e.m. for data pooled from three or more independent experiments. (D) SOX10 (green), PAX7 (red) and TFAP2A (turquoise) triple labeling of D5+CHIR cultures treated with increasing amount of BMP4 administered from day 0 to day 1.

We further performed a BMP-titration assay to better define the role of BMP in NC induction. Expression of SOX10, PAX7 and TFAP2A displayed no obvious gains or losses upon BMP4 addition from day 0 to day 1 at a dosage range of 0.005-0.01 ng/ml. However, at 0.05 ng/ml BMP4 or above, expression of SOX10 and PAX7 was severely reduced, whereas TFAP2A expression was detected ubiquitously, suggestive of non-neural ectoderm identity (Fig. 5D).

Human NC cells form independently of PAX6$^+$ neuroectoderm

NC cells are believed to derive from neural plate cells, but avian experiments have suggested an independent origin (Basch et al., 2006), and the early requirement for BMP signaling in human NC induction also deviates from this notion. The neural induction program in human embryos and ESCs has been studied (Greber et al., 2011; Hou et al., 2013; Zhang et al., 2010). Although there was transient and variable upregulation of the pluripotency/neural markers *SOX2*, *SOX1* and *OTX2* during our NC cell induction, other pre-neural and mature neural progenitor markers, such as *LHX2* and *HES5*, were never induced (data not shown; Fig. S4A,B). Our results do not support a robust execution of the pre-neural and neural program during induction of human NC cells.

PAX6 has been proposed as the earliest definitive neuroectoderm marker in human embryos and ESCs (Chambers et al., 2009; Gerrard et al., 2005; Surmacz et al., 2012; Zhang et al., 2010). We performed triple labeling of OCT4, PAX6 and SOX10 in day 1, day 3 and day 5 control and CHIR-treated cultures, to denote ESC, neuroectoderm and NC fates, respectively (Fig. 6A). Under control (−CHIR) and NC-inducing (+CHIR) treatments, we observed progressive reduction of OCT4$^+$ cells from day 1 to day 5. A small amount of PAX6$^+$ cells were induced in the control cultures starting at day 3 but there was no further increase of PAX6$^+$ cells at day 5, consistent with our findings that control cultures mainly formed non-neural cell types. Similar to control cultures, in the presence of CHIR, minimal PAX6$^+$ cells ($\leq$5%) were induced at all time points. Some SOX10$^+$ cells ($\sim$10% of the total population), however, started to arise at day 3. By day 5, the number of SOX10$^+$ cells climbed to $\sim$60% or higher but the number of PAX6$^+$ cells barely reached 5% of the total population (Fig. 6A,B). No co-expression or spatial relationship of the SOX10$^+$ and the small population of PAX6$^+$ cells were noted at day 5. To address possible contributions of PAX6 in the CHIR-mediated NC induction, we performed PAX6-knockdown

Development (2016) 143, 398-410 doi:10.1242/dev.130849

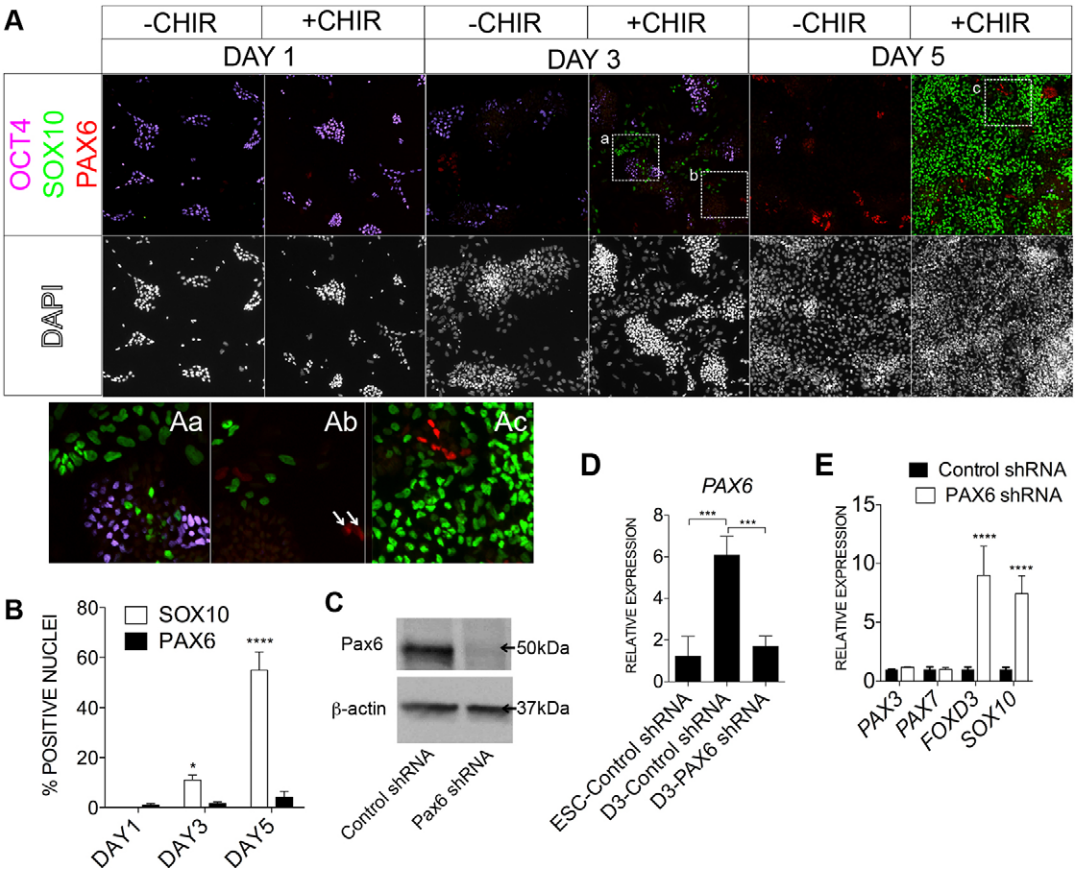

Fig. 6. WNT-induced human NC cells arise independently of PAX6$^+$ neuroepithelial cells. (A) Immunostaining of OCT4 (violet), SOX10 (green) and PAX6 (red) in day 1, day 3 and day 5 cultures treated with (+) or without (–) CHIR. Framed regions, from day 3 (Aa, Ab) and day 5 (Ac) cultures are shown as magnified images; arrows highlight the few PAX6$^+$ cells in day 3 +CHIR cultures. (B) Quantification of SOX10$^+$ and PAX6$^+$ nuclei in day 1, 3 and 5 cultures treated with CHIR. (C) Western blot of PAX6 protein in control and *PAX6* shRNA-treated cells, with ladder sizes indicated. (D,E) Quantitative gene expression analysis showing effective knockdown of *PAX6* at day 3 (D), but no reduction of NC markers at day 5 in *PAX6*-specific shRNA-treated cells (E). *P≤0.05, ***P≤0.001, ****P≤0.0001. Error bars represent s.d.

experiments. Application of *PAX6* shRNA to CHIR-treated cells led to robust reduction of *PAX6* protein and transcript (Fig. 6C,D). Notably, PAX6 knockdown cultures did not exhibit a reduction in NC markers and, instead, selected markers such as *SOX10* and *FOXD3* displayed higher expression (Fig. 6E; data not shown). We conclude that human NC cells can be generated independently of PAX6$^+$ neuroectoderm cells.

Endogenous FGF signaling is required for NC induction, and exogenous FGF triggers mesoderm character

FGF signaling has been implicated in NC induction in animal models, either acting directly on NC precursors or via mesoderm induction (Mayor et al., 1997; Stuhlmiller and Garcia-Castro, 2012b; Yardley and Garcia-Castro, 2012). Treatment of differentiating hESCs with PD 173074, an FGFR1- and FGFR3-specific inhibitor, repressed the expression of the FGF targets *SPRY1* and *SPRY2* by 40-50% (Fig. 7A). Examination of NC markers at differentiation day 5 revealed decreased expression of all examined NC genes when PD 173074 was administered continuously for 5 days (Fig. 7B), suggesting that FGF signaling is required for human NC induction in accordance with previous findings from animal models (Stuhlmiller and Garcia-Castro, 2012b).

WNT signaling is known to promote mesoderm induction in differentiating hESCs (Funa et al., 2015; Sumi et al., 2008). We found that *T* transcription (brachyury, a marker of mesoderm) was transiently upregulated in our cultures, peaking at day 3 (~10-fold compared with undifferentiated ESCs), before returning to undifferentiated levels at day 5 (Fig. S4C). Transcription of *T*, as well as another mesoderm marker, *TBX6*, could be promoted by the presence of FGF2, consistent with the role of FGF signaling in mesoderm induction (Fig. 7C; data not shown) (Vallier et al., 2009). Despite detectable *T* transcription, T$^+$ cells were not detected in our differentiating cultures, whereas CHIR plus FGF2 treatment readily induced T$^+$ cell clusters (~5% of the cell clusters; Fig. 7D). There was also no evidence of robust transcriptional upregulation of other mesoderm precursor or progenitor markers during CHIR-induced differentiation (e.g. *MIXL1*, *MESP1*, cardiac-specific *NKX2-5*) (Fig. S4D; data not shown). The induction of T$^+$ cells upon FGF treatment supports the idea that mesoderm induction in our system requires exogenous FGF signals.

Human NC cells differentiate via an early pre-border state with distinct signaling requirements from the neural plate border

In chick embryos, the earliest NC marker identified with a restricted expression at the border of the forming neural plate is PAX7 (Basch et al., 2006). Our unpublished results in rabbit and mouse embryos support Pax7 association with early NC development in mammals.

Development (2016) 143, 398-410 doi:10.1242/dev.130849

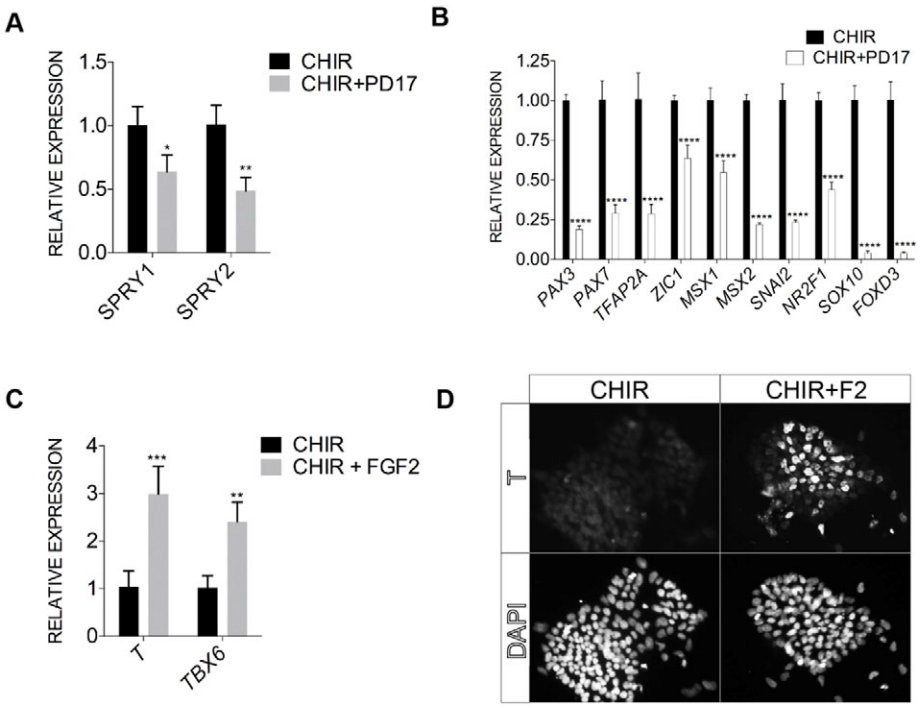

Fig. 7. Exogenous and endogenous FGF signaling is required for mesoderm and NC induction, respectively. (A,B) Quantitative gene expression analysis for the effects of the FGF inhibitor PD 173074 (PD17, 200 nM) on the FGF targets *SPRY1* and *SPRY2* (D3+CHIR cultures; A) and NC markers (D5+CHIR; B). (C) Quantification of brachyury (*T*) and *TBX6* expression in day 3 CHIR-treated cultures alone, or supplemented with 20 ng/ml FGF2 (CHIR+FGF2) from day 0 to 3. (D) Brachyury (T) immunostaining of day 3 +CHIR cultures alone or supplemented with 20 ng/ml of FGF2 (CHIR+F2) from day 0 to day 3. Error bars represent s.d.; three independent culture experiments were performed and data from one representative experiment are shown. *$P\leq0.05$, **$P\leq0.01$, ***$P\leq0.001$, ****$P\leq0.0001$.

We performed co-labeling of PAX7 and OCT4 to assess the transition of hESCs to PAX7$^+$ NC progenitors and found PAX7$^+$OCT4$^+$ and PAX7$^+$OCT4$^-$ cell populations in the day 3 cultures (Fig. 8A, yellow arrows and white arrowheads, respectively). Interestingly, the majority of cells expressing a high level of PAX7 displayed no or very low OCT4. We proposed that during the WNT-induction of human NC cells, differentiating hESC might transit from OCT4$^+$ ESCs to OCT4^{low}PAX7^{low} cells, before acquiring an OCT4$^-$PAX7$^+$ status associated with a NC progenitor stage.

As a first step aiming to identify earlier events during NC induction that might precede the OCT4-PAX7 transition, we focused on genes functionally involved in early NC induction in animal models. Gain- and loss-of-function experiments in frog embryos reveal early functions of Gbx2 and Sp5 in the NC induction cascade and in the regulation of neural plate border gene expression (Li et al., 2009; Park et al., 2013). *Gbx2*$^{-/-}$ mice display a reduction of post-otic NC cells and a NC migration patterning defect (Byrd and Meyers, 2005). We found that both were specifically induced by CHIR (Fig. 8B,C). Their expression peaked at differentiation day 2 and day 3, respectively. Overexpression of Zic3 induces ectopic NC tissues in amphibian embryos (Nakata et al., 1997) and is suggested to be an early NC specifier in teleost embryos (Garnett et al., 2012). We found that *ZIC3* was transiently induced during differentiation either in the presence or absence of CHIR (Fig. 8D). CHIR, however, promoted a further increase/maintenance of *ZIC3*, which peaked at differentiation day 2. *ZEB2*, a causative gene in human Hirschsprung's disease associated with failure to form NC-derived enteric ganglia (Wakamatsu et al., 2001) that is expressed very early in the developing mouse neural fold and NC (Miyoshi et al., 2006; Van de Putte et al., 2003), was specifically induced by CHIR (Fig. 8E). Similar to *GBX2*, *SP5* and *ZIC3*, *ZEB2* expression peaked between differentiation day 2 and day 3. We consequently dubbed these genes as pre-neural plate border or simply 'pre-border' (pB) genes because their induction and peak of expression preceded the classical neural plate border genes such as *PAX7*, *PAX3*, *MSX1* and *TFAP2A* (Fig. 1G; Fig. 3D).

Because pB genes and 'neural border' (NB) genes were induced with different temporal kinetics, we wished to test whether these two gene groups were differentially regulated. We therefore examined the response of pB (*GBX2*, *SP5*, *ZIC3* and *ZEB2*) and NB (*PAX3*, *PAX7*, *MSX1* and *TFAP2A*) genes to alterations of WNT, BMP and FGF signaling. Knocking down *CTNNB1* by shRNA consistently inhibited expression of all pB and NB genes, except *TFAP2A* (which was also expressed highly in control non-neural ectoderm cultures) (Fig. 8F), suggesting that most, if not all, pB and NB genes were regulated by WNT/CTNNB1 signaling. Intriguingly, blocking BMP signaling with noggin did not affect expression of pB genes, but significantly repressed all NB genes (Fig. 8G). Addition of FGF2 ligand also inhibited expression of all NB genes, but had little effect on pB genes except *GBX2* (Fig. 8H). In conclusion, we propose that human NC induction undergoes a stage-wise progression following a sequence of pB, NB and mature NC stages, with pB genes mainly regulated by canonical WNT signaling and partially by FGF signaling but not by BMP signaling (Fig. 8I).

DISCUSSION

hESCs resemble mouse epiblast stem cells in terms of signaling requirements and gene regulatory network for self-renewal and maintenance. The exact embryonic equivalent of ESCs in humans, however, is still under debate. hESCs appear to display low but heterogeneous endogenous WNT activity (Blauwkamp et al., 2012; Davidson et al., 2012). The absolute requirement of WNT activity in hESC renewal is contested but it appears that nuclear β-catenin signaling is dispensable for ESC maintenance (Kim et al., 2013) and WNT activation leads to differentiation of hESCs (Davidson et al., 2012; Dravid et al., 2005). Combining various chemically defined conditions, cell plating strategies, and activation of signaling pathways, such as activin, Nodal and FGF, WNT activation via GSK3 inhibition or constitutively active β-catenin can direct the differentiation of hESCs into a number of embryonic cell types, including

Development (2016) 143, 398-410 doi:10.1242/dev.130849

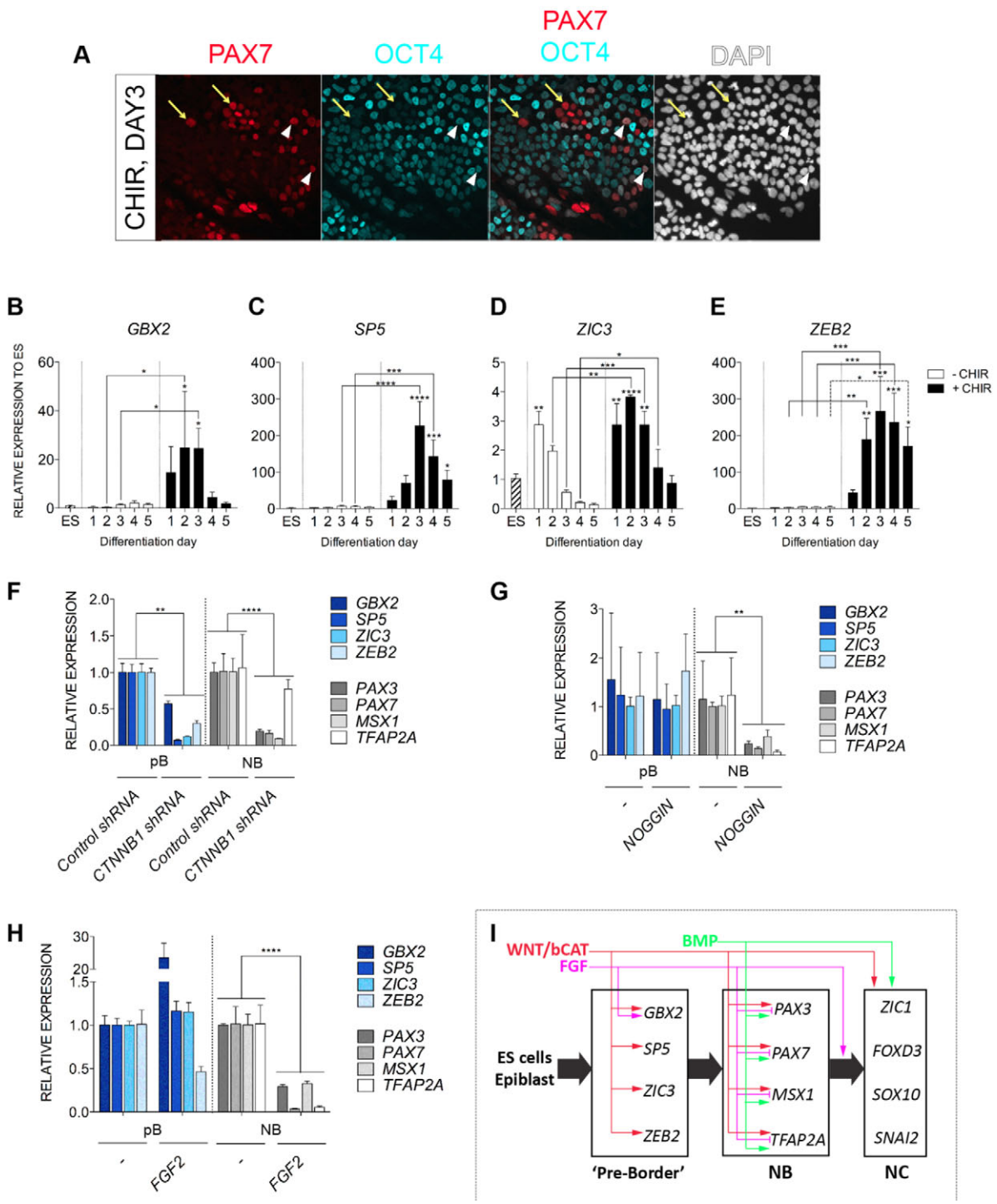

Fig. 8. Identification of a class of early pre-border genes and their signaling requirements for expression. (A) Double immunostaining of PAX7 (red) and OCT4 (turquoise) in day 3 +CHIR cultures. Yellow arrows denote nuclei expressing PAX7 but with no OCT4 staining. White arrowheads indicate nuclei expressing PAX7 and OCT4. (B-E) Time course of quantitative gene expression analysis of *GBX2*, *SP5*, *ZIC3* and *ZEB2* in ESCs (ES), control cultures (−CHIR) and with CHIR-treated (+CHIR) cultures. (F-H) Differential response of pre-neural border (pB: *GBX2*, *SP5*, *ZIC3*, *ZEB2*) and neural border genes (NB: *PAX7*, *PAX3*, *MSX1*, *TFAP2A*) genes to WNT, BMP and FGF signaling analyzed by RT-PCR in D3+CHIR cultures exposed to specific modulators. Statistical analyses were carried out using two-way ANOVA with Fisher's tests. β-catenin knockdown (CTNNB1 shRNA) leads to reduced expression of both pB and NB genes (F). BMP inhibition (NOG, from day 0 to day 1) represses NB but not pB genes (G). FGF modulation by FGF2 ligand led to enhanced or unaffected pB expression and reduced NB expression (H). (I) A step-wise induction model for human NC and a gene regulatory network of human NC with signaling inputs from canonical WNT, FGF and BMP signaling. *$P\leq0.05$, **$P\leq0.01$, ***$P\leq0.001$, ****$P\leq0.0001$.

primitive streak/mesendoderm (Funa et al., 2015; Gouti et al., 2014; Nakanishi et al., 2009; Sumi et al., 2008; Tsakiridis et al., 2015), paraxial mesoderm (Shelton et al., 2014; Tan et al., 2013; Umeda et al., 2012), lateral plate mesoderm (Tan et al., 2013), caudal neural plate, and axial stem cell progenitors (Denham et al., 2015; Tsakiridis et al., 2015).

Development (2016) 143, 398-410 doi:10.1242/dev.130849

Here, we report a robust and efficient method of inducing NC cells from hESCs. Our approach is based on (1) a precise seeding density of dissociated hESCs, (2) a defined medium composition, and (3) the small molecule GSK inhibitor CHIR 99021 to activate WNT signaling. Through this protocol, hESCs sequentially lose stemness/pluripotency markers and acquired characteristics of NC cells. We found that markers associated with non-neural ectoderm, placodal and epidermal tissues arise in the absence of WNT induction, as suggested by a previous study (Leung et al., 2013). WNT activation instead represses the non-neural ectoderm program and promotes NC induction. Using knockdown assays, we demonstrated that β-catenin is responsible for the activation of a set of early pB genes largely independently of BMP or FGF signaling. Interestingly, during *in vitro* hESC differentiation into primitive streak and NC precursors, β-catenin binding was observed in the genomic regions close to, or within the loci of, all four pre-border genes *GBX2*, *SP5*, *ZEB2* and *ZIC3* (Funa et al., 2015). Our findings are also in line with our previous work in the amniote avian embryo, which develops from a flat blastodisc in a similar manner to humans and most mammals. Through fate-mapping and specification assays, we proposed that the earliest NC populations arise independently of neural and mesodermal tissues, from precursors that precede the standard neural plate border characteristics (Basch et al., 2006).

The 'binary competence' model of neural crest/cranial placode induction proposed a segregation of NC and cranial placode competence at the neural plate border stage (Schlosser, 2008). Contrary to this model, we found that WNT directs a segregation of early NC and cranial placode cell fates prior to the induction of the neural plate border markers; pB genes such as *GBX2*, *ZEB2*, *SP5* and *ZIC3* are induced by WNT/CTNNB1 signaling 1 or 2 days prior to induction of the NB genes *PAX3*, *PAX7* and *MSX1*. Moreover, expression of neural border markers common to both NC and cranial placodes, such as *TFAP2A* and *ZIC1*, displayed distinct kinetics during the course of human NC and cranial placode induction (Fig. 3D,E; Leung et al., 2013) further supporting the idea that segregation of NC and cranial placode fates occurs very early in our cultures. It has been suggested that NC competence segregates with the neuralized domain of the ectoderm (Pieper et al., 2012; Schlosser, 2008). We have examined the expression dynamics of a number of neural-related transcripts, including *LHX2*, *PAX6*, *SOX1*, *SOX2*, *OTX2* and *HES5* (Greber et al., 2011; Hou et al., 2013; Zhang et al., 2010). Variable and mild (~10-fold or less) increases in expression were observed in only a subset of these genes (*PAX6*, *SOX1*, *SOX2*, *OTX2*) and others were not induced at all (*LHX2* and *HES5*). Time course antibody staining for PAX6 also revealed minimal induction of $PAX6^+$ cells and, most importantly, we did not observe any correlation in time and space for the induction of $PAX6^+$ cells and $SOX10^+$ NC cells. Furthermore, knockdown assays also suggested that reduced PAX6 function did not negatively interfere with NC induction. An early origin of human NC cells independent of neural progenitors has been suspected (Chambers et al., 2013), and our embryological evidence has also suggested the capacity of non-neural ectoderm to form NC without acquiring a neural character (Yardley and Garcia-Castro, 2012). Our data substantiate this notion by showing that human NC cells form independently of $PAX6^+$ neuroectoderm.

Neural induction in hESCs requires inhibition of either BMP or activin, or both (Chambers et al., 2009; Pera et al., 2004; Smith et al., 2008; Surmacz et al., 2012). The fact that administration of noggin blocked expression of NC and/or neural border markers suggests that human NC induction requires BMP activation, which is distinct from neural induction. The effect of noggin on NC induction appears to be delayed as treatment of noggin from day 0 to day 1 did not translate into repression of pB genes as only NB genes were blocked. It is also worth noting that transcripts for BMP ligands including *BMP2*, *BMP4* and *BMP7*, can be readily detected under CHIR treatment (data not shown), supporting the suggested contribution of this pathway during later events in NC development (Faure et al., 2002; Liem et al., 1997, 1995; Selleck and Bronner-Fraser, 1995; Stuhlmiller and Garcia-Castro, 2012b).

Alternative neural induction pathways have been proposed. For instance, induction of human neural tube cells posterior to the forebrain has been shown to require endogenous WNT ligand activity (Lupo et al., 2013). Also, retinoic acid/FGF activity can posteriorize human neural progenitors, consistent with the roles proposed for these signaling pathways in animal models. We observed robust induction of engrailed 1 (*EN1*), but not caudal HOX genes, suggesting that our cultures might have induced cells equivalent to those that reside at the mid/hindbrain level (data not shown). Pre-migratory NC and dorsal neural tube cells share expression of a number of genes, including *En1*, *Bmp4*, *Bmp7*, *Wnt1*, *Wnt3*, *Mafb* and *Lmx1a* (Krispin et al., 2010). However, as discussed above, our cultures did not display definitive features of neural precursors. Furthermore, we obtained high yields of $SOX10^+PAX7^+TFAP2A^+$ triple-labeled cells. These observations argue against a co-induction of a substantial percentage of dorsal neural tube progenitors in our cultures.

Our study established a rapid (5 days) and efficient protocol for generating a high yield of NC cells. Other studies have relied on surface markers such as HNK1 (human natural killer-1) and p75NTR (NGFR) (Fukuta et al., 2014; Jiang et al., 2009; Lee et al., 2010, 2007; Menendez et al., 2011; Umeda et al., 2012), that are respectively known to label only few human NC cells or to have robust expression in non-NC cell populations (Betters et al., 2010). We instead relied on PAX7, TFAP2A and SOX10, which have been identified as robust markers co-expressed in a specific fashion in embryonic human NC (Betters et al., 2010). Our protocol simplifies previous approaches by eliminating the use of the BMP inhibitor noggin and/or the activin receptor inhibitor SB 431542. By modulating the initial seeding density thereby allowing efficient induction in the absence of a pre-differentiation period (Chambers et al., 2013; Fukuta et al., 2014; Menendez et al., 2011; Mica et al., 2013; Umeda et al., 2012), we attempt to limit the possible effects of paracrine signals of unknown nature that are produced by neighboring cells, and provide a sensitive model responsive to engineered cues for development. Simultaneously, we significantly shorten the total length of time required for the induction protocol [from ~9 days with the current shortest protocol (Fukuta et al., 2014) to 5 days with our protocol]. Our newly devised protocol appears to be a useful supplement to the current induction protocols in generating human NC cells, and will certainly facilitate future studies on human NC development.

MATERIALS AND METHODS

hESC/iPSC growth and maintenance

WA01 (WiCell), WA09 (WiCell), Y6 iPSC (Yale Stem Cell Center) and RIV9 iPSCs (University of California Riverside) of passages 30 to 70 were maintained on plastic surfaces coated with Matrigel (08-774-552, Fisher Scientific) in serum-free medium (mTeSR1, STEMCELL Technologies). Cultures were passaged every 6 to 7 days using Dispase (STEMCELL Technologies) according to the manufacturer's instructions.

Neural crest cell induction

Human ESC/iPSC colonies digested with Accutase cell detachment solution (Innovative Cell Technologies) were re-suspended in differentiation

Development (2016) 143, 398-410 doi:10.1242/dev.130849

medium plus CHIR 99021 (3 µM; #4423 Tocris Bioscience) plated at the indicated densities on Matrigel-coated surfaces. Differentiation medium contained DMEM/F12 medium supplemented with 2% B27 supplement (Life Technologies), 1× Glutamax (Life Technologies) and 0.5% bovine serum albumin (wt/vol) (A9647, Sigma-Aldrich). The ROCK inhibitor Y-27632 (10 µM; Tocris Bioscience) was added for the first two days. Noggin (300-500 ng/ml; R&D systems), BMP4 (0.001-20 ng/ml; R&D Systems), SB 431542 (20 µM; Tocris Bioscience), FGF2 (5-20 ng/ml; R&D Systems), PD 173074 (200 nM; Tocris) and PD 184352 (5 µM; Tocris) were added as indicated. Small molecules and medium were replenished daily.

Neural crest cell differentiation

Day 5 CHIR-treated cells were plated at 20,000-80,000 cells/cm^2 on a Matrigel-coated surface with NC induction medium, supplemented with 10 µM Y-27632 overnight. Medium was changed by 24 h post-plating to terminal differentiation media. For peripheral neurons, melanoblasts and glial progenitors, differentiation medium contained DMEM/F12 with 2% B27 supplement, 1× Glutamax, 3 µM CHIR 99021, 1 µM SU-5402 (Tocris) and 2.5 µM N-[N-(3,5-difluorophenacetyl)-L-alanyl]-S-phenylglycine t-butyl ester (DAPT; Calbiochem, 565784; 10 µM). For osteoblast differentiation, medium contained 50 mg/ml ascorbic acid, 10 mM β-glycerophosphate and 50 nM 1α,25-OH vitamin D3 (zur Nieden et al., 2003). Media were changed every 3-4 days. Cultures were harvested at the indicated time and processed for Alizarin Red staining. For chondrocyte differentiation, dissociated day 5 cells were pelleted at 1200 rpm (280 ***g***) at a concentration of 1×10^6 cells/ml and incubated in 1 ml of MesenCult-ACF Chondrogenic Differentiation Medium (05455; Stem Cell Technologies). Cells were fed every 3-5 days. At day 21, pellets were fixed with 10% formalin or 4% paraformaldehyde, paraffin sectioned and processed for Alcian Blue staining.

Transcript analyses

Total RNAs were extracted using TRIzol reagent (Life Technologies). Total RNA (0.5-1 µg) was reverse-transcribed using SMART MMLV reverse transcriptase (Clontech Laboratories). Real-time polymerase chain reaction (PCR) was carried out using the iTaq universal SYBR Green supermix (Bio-Rad) and the IQ5 Real-Time PCR Detection System (Bio-Rad). The primer concentration was 160 nM. Forty cycles of reactions were performed followed by melt curves to confirm specificity of primer sets. Three to six biological replicates were measured. Primer sequences are listed in Table S1.

Lentiviral constructs

Human shRNA sequences for *CTNNB1* and *PAX6* were designed using a set of rules that maximize knockdown efficiency and minimize off-targets (http://www.broadinstitute.org/rnai/public/resources/rules). These sequences were retrieved from the RNAi consortium database (http://www.broadinstitute.org/rnai/public/). Target sequences tested are listed in Table S2. Annealed shRNA oligos with the loop sequence TTCAAGAGA are cloned between the *Age*I and *Eco*RI sites of pLKO.1 puro (a gift from Bob Weinberg, plasmid #8453, Addgene) (Stewart et al., 2003).

Generation of lentivirus and stable hESC lines

For lentivirus generation, the helper constructs psPAX2 and pMD2.G (both a gift from Didier Trono, plasmids #12260 and #12259, respectively, Addgene) together with the transfer vector were transfected into the 293T/17 cell line (CRL-11268, ATCC) using the calcium phosphate precipitation method. Viruses were partially purified using Lenti-X concentrator (Clontech Laboratories). For lentivirus infection, WA01 ESCs, plated at 20,000 cells/cm^2 were incubated in mTeSR1 medium (STEMCELL Technologies) containing titrated amount of concentrated lentivirus and polybrene (6 µg/ml) for 4-8 h. Antibiotic selection began at 48 h post infection with puromycin (Tocris, 4089) at 1 µg/ml.

Immunofluorescence

Immunofluorescence was performed on cells cultured on Nunc Lab-Tek Chamber Slide System (Thermo Scientific, # 177399). Cultures were fixed (4% paraformaldehyde, 12 min), permeabilized (0.4% Tween-20, 12 min) and blocked (10% fetal bovine serum, 1 h) at room temperature. Primary antibody and secondary antibody incubation were performed in 4% fetal bovine serum overnight at 4°C and 1 h at room temperature, respectively. Primary antibodies are listed in Table S3. Secondary antibodies were species- or subtype-specific Alexa secondary antibodies (Life Technologies). Images were taken using a Nikon Eclipse 80i microscope and a SPOT cooled camera or a Zeiss M1 imager. Images were processed in Adobe Photoshop CC version 14.2.1. and were adjusted simultaneously in exactly the same manner for experimental and control sets.

Western blotting

Cells were lysed using RIPA lysis buffer (50 mM Tris-HCl pH 7.4, 150 mM NaCl, 5 mM EDTA, 0.5% sodium deoxycholate, 1% Igepal, 0.1% SDS), plus protease inhibitors (Roche Diagnostics), followed by sonification and centrifugation to remove cell debris. Protein quantification was performed using the Quick Start Bradford Protein Assay (Bio-Rad). Ten-µg protein samples in Lammeli buffer with DTT were separated on a 12% SDS-PAGE gel and transferred to PVDF membrane (Bio-Rad). Membrane was blocked with 5% milk and incubated with the primary antibodies mouse monoclonal anti-β-catenin (610153, BD Biosciences; 1:2000), mouse IgG1 anti-PAX6 (Developmental Studies Hybridoma Bank; 1:500) or mouse monoclonal anti-β-actin (A5316, Sigma-Aldrich; 1:10,000) for 1 h at room temperature. Membrane was then incubated with a horseradish peroxidase-conjugated secondary antibody goat anti-mouse IgG (H+L) (Thermo Fisher Scientific, 31432). Signal was developed using the Clarity Western ECL Kit (Bio-Rad) and detected using x-ray films.

Statistical analyses

Chart drawing and statistical analyses were performed using the GraphPad software Prism (version 6.0f). Asterisks indicate statistical significance: *$P\leq0.05$, **$P\leq0.01$, ***$P\leq0.001$, ****$P\leq0.0001$. Unpaired *t*-tests and one-way ANOVA tests were respectively performed for comparisons of two or more means.

Acknowledgements

We thank Dr zur Nieden and Nicole Sparks (UCR) for osteogenic culture assistance, Yale undergraduate helpers Laura Miyares, Cayla Broton and Kevin Kwang for assistance in cell counting and real-time PCR analyses, and the Valerie Horsley laboratory for the maintenance of the stem cell facility. WA01 and WA09 cell lines were obtained from the WiCell Institute through the Yale Stem Cell Center. The monoclonal antibodies against TFAP2A (3B5), PAX6 and PAX7 were obtained from the Developmental Studies Hybridoma Bank developed under the auspices of the National Institute of Child Health and Human Development and maintained by the University of Iowa, Department of Biology, Iowa City, IA 52242, USA.

Competing interests

The authors declare no competing or financial interests.

Author contributions

M.I.G.-C. conceived and directed the study. A.W.L. and B.M. established and optimized the differentiation protocol. A.W.L. performed most of the experiments. A.F.M., M.S.P. and G.A.G. assisted with western blots, iPS NC derivation, and terminal derivative experiments. A.W.L., A.F.M., M.S.P., G.A.G. and M.I.G.-C. analyzed data. A.W.L. and M.I.G.-C. wrote the manuscript and generated figures. All authors proofread and approved the final manuscript.

Funding

This work is supported by funding from the National Institutes of Health National Institute of Dental and Craniofacial Research [2R01DE017914]; and Connecticut Innovations [14-SCB-YALE11]. Deposited in PMC for release after 12 months.

Supplementary information

Supplementary information available online at
http://dev.biologists.org/lookup/suppl/doi:10.1242/dev.130849/-/DC1

References

Baker, C. V. H. and Bronner-Fraser, M. (1997). The origins of the neural crest. Part II: an evolutionary perspective. *Mech. Dev.* **69**, 13-29.

Barriga, E. H., Trainor, P. A., Bronner, M. and Mayor, R. (2015). Animal models for studying neural crest development: is the mouse different? *Development* **142**, 1555-1560.

Basch, M. L., Bronner-Fraser, M. and Garcia-Castro, M. I. (2006). Specification of the neural crest occurs during gastrulation and requires Pax7. *Nature* **441**, 218-222.
Betters, E., Liu, Y., Kjaeldgaard, A., Sundstrom, E. and Garcia-Castro, M. I. (2010). Analysis of early human neural crest development. *Dev. Biol.* **344**, 578-592.
Blauwkamp, T. A., Nigam, S., Ardehali, R., Weissman, I. L. and Nusse, R. (2012). Endogenous Wnt signalling in human embryonic stem cells generates an equilibrium of distinct lineage-specified progenitors. *Nat. Commun.* **3**, 1070.
Buitrago-Delgado, E., Nordin, K., Rao, A., Geary, L. and LaBonne, C. (2015). Shared regulatory programs suggest retention of blastula-stage potential in neural crest cells. *Science* **348**, 1332-1335.
Byrd, N. A. and Meyers, E. N. (2005). Loss of Gbx2 results in neural crest cell patterning and pharyngeal arch artery defects in the mouse embryo. *Dev. Biol.* **284**, 233-245.
Chambers, S. M., Fasano, C. A., Papapetrou, E. P., Tomishima, M., Sadelain, M. and Studer, L. (2009). Highly efficient neural conversion of human ES and iPS cells by dual inhibition of SMAD signaling. *Nat. Biotechnol.* **27**, 275-280.
Chambers, S. M., Mica, Y., Lee, G., Studer, L. and Tomishima, M. J. (2013). Dual-SMAD inhibition/WNT activation-based methods to induce neural crest and derivatives from human pluripotent stem cells. *Methods Mol. Biol.* **1307**, 329-343.
Davidson, K. C., Adams, A. M., Goodson, J. M., McDonald, C. E., Potter, J. C., Berndt, J. D., Biechele, T. L., Taylor, R. J. and Moon, R. T. (2012). Wnt/beta-catenin signaling promotes differentiation, not self-renewal, of human embryonic stem cells and is repressed by Oct4. *Proc. Natl. Acad. Sci. USA* **109**, 4485-4490.
de Croze, N., Maczkowiak, F. and Monsoro-Burq, A. H. (2011). Reiterative AP2a activity controls sequential steps in the neural crest gene regulatory network. *Proc. Natl. Acad. Sci. USA* **108**, 155-160.
Denham, M., Hasegawa, K., Menheniott, T., Rollo, B., Zhang, D., Hough, S., Alshawaf, A., Febbraro, F., Ighaniyan, S., Leung, J. et al. (2015). Multipotent caudal neural progenitors derived from human pluripotent stem cells that give rise to lineages of the central and peripheral nervous system. *Stem Cells* **33**, 1759-1770.
Dincer, Z., Piao, J., Niu, L., Ganat, Y., Kriks, S., Zimmer, B., Shi, S.-H., Tabar, V. and Studer, L. (2013). Specification of functional cranial placode derivatives from human pluripotent stem cells. *Cell Rep.* **5**, 1387-1402.
Dravid, G., Ye, Z., Hammond, H., Chen, G., Pyle, A., Donovan, P., Yu, X. and Cheng, L. (2005). Defining the role of Wnt/beta-catenin signaling in the survival, proliferation, and self-renewal of human embryonic stem cells. *Stem Cells* **23**, 1489-1501.
Evans, M. (2011). Discovering pluripotency: 30 years of mouse embryonic stem cells. *Nat. Rev. Mol. Cell Biol.* **12**, 680-686.
Faure, S., de Santa Barbara, P., Roberts, D. J. and Whitman, M. (2002). Endogenous patterns of BMP signaling during early chick development. *Dev. Biol.* **244**, 44-65.
Fukuta, M., Nakai, Y., Kirino, K., Nakagawa, M., Sekiguchi, K., Nagata, S., Matsumoto, Y., Yamamoto, T., Umeda, K., Heike, T. et al. (2014). Derivation of mesenchymal stromal cells from pluripotent stem cells through a neural crest lineage using small molecule compounds with defined media. *PLoS ONE* **9**, e112291.
Funa, N. S., Schachter, K. A., Lerdrup, M., Ekberg, J., Hess, K., Dietrich, N., Honore, C., Hansen, K. and Semb, H. (2015). β-Catenin regulates primitive streak induction through collaborative interactions with SMAD2/SMAD3 and OCT4. *Cell Stem Cell* **16**, 639-652.
Gans, C. and Northcutt, R. G. (1983). Neural crest and the origin of vertebrates: a new head. *Science* **220**, 268-273.
Garcia-Castro, M. I., Marcelle, C. and Bronner-Fraser, M. (2002). Ectodermal Wnt function as a neural crest inducer. *Science* **297**, 848-851.
Garnett, A. T., Square, T. A. and Medeiros, D. M. (2012). BMP, Wnt and FGF signals are integrated through evolutionarily conserved enhancers to achieve robust expression of Pax3 and Zic genes at the zebrafish neural plate border. *Development* **139**, 4220-4231.
Gerrard, L., Rodgers, L. and Cui, W. (2005). Differentiation of human embryonic stem cells to neural lineages in adherent culture by blocking bone morphogenetic protein signaling. *Stem Cells* **23**, 1234-1241.
Gouti, M., Tsakiridis, A., Wymeersch, F. J., Huang, Y., Kleinjung, J., Wilson, V. and Briscoe, J. (2014). In vitro generation of neuromesodermal progenitors reveals distinct roles for wnt signalling in the specification of spinal cord and paraxial mesoderm identity. *PLoS Biol.* **12**, e1001937.
Greber, B., Coulon, P., Zhang, M., Moritz, S., Frank, S., Muller-Molina, A. J., Arauzo-Bravo, M. J., Han, D. W., Pape, H.-C. and Scholer, H. R. (2011). FGF signalling inhibits neural induction in human embryonic stem cells. *EMBO J.* **30**, 4874-4884.
Groves, A. K. and LaBonne, C. (2014). Setting appropriate boundaries: fate, patterning and competence at the neural plate border. *Dev. Biol.* **389**, 2-12.
Hong, C.-S. and Saint-Jeannet, J.-P. (2007). The activity of Pax3 and Zic1 regulates three distinct cell fates at the neural plate border. *Mol. Biol. Cell* **18**, 2192-2202.
Hou, P.-S., Chuang, C.-Y., Kao, C.-F., Chou, S.-J., Stone, L., Ho, H.-N., Chien, C.-L. and Kuo, H.-C. (2013). LHX2 regulates the neural differentiation of human embryonic stem cells via transcriptional modulation of PAX6 and CER1. *Nucleic Acids Res.* **41**, 7753-7770.
Jiang, X., Gwye, Y., McKeown, S. J., Bronner-Fraser, M., Lutzko, C. and Lawlor, E. R. (2009). Isolation and characterization of neural crest stem cells derived from in vitro-differentiated human embryonic stem cells. *Stem Cells Dev.* **18**, 1059-1071.
Kim, H., Wu, J., Ye, S., Tai, C.-I., Zhou, X., Yan, H., Li, P., Pera, M. and Ying, Q.-L. (2013). Modulation of beta-catenin function maintains mouse epiblast stem cell and human embryonic stem cell self-renewal. *Nat. Commun.* **4**, 2403.
Krispin, S., Nitzan, E. and Kalcheim, C. (2010). The dorsal neural tube: a dynamic setting for cell fate decisions. *Dev. Neurobiol.* **70**, 796-812.
Kwon, H.-J., Bhat, N., Sweet, E. M., Cornell, R. A. and Riley, B. B. (2010). Identification of early requirements for preplacodal ectoderm and sensory organ development. *PLoS Genet.* **6**, e1001133.
Lee, G., Kim, H., Elkabetz, Y., Al Shamy, G., Panagiotakos, G., Barberi, T., Tabar, V. and Studer, L. (2007). Isolation and directed differentiation of neural crest stem cells derived from human embryonic stem cells. *Nat. Biotechnol.* **25**, 1468-1475.
Lee, G., Chambers, S. M., Tomishima, M. J. and Studer, L. (2010). Derivation of neural crest cells from human pluripotent stem cells. *Nat. Protoc.* **5**, 688-701.
Leung, A. W., Kent Morest, D. and Li, J. Y. H. (2013). Differential BMP signaling controls formation and differentiation of multipotent preplacodal ectoderm progenitors from human embryonic stem cells. *Dev. Biol.* **379**, 208-220.
Li, B., Kuriyama, S., Moreno, M. and Mayor, R. (2009). The posteriorizing gene Gbx2 is a direct target of Wnt signalling and the earliest factor in neural crest induction. *Development* **136**, 3267-3278.
Liem, K. F., Jr., Tremml, G., Roelink, H. and Jessell, T. M. (1995). Dorsal differentiation of neural plate cells induced by BMP-mediated signals from epidermal ectoderm. *Cell* **82**, 969-979.
Liem, K. F., Jr., Tremml, G. and Jessell, T. M. (1997). A role for the roof plate and its resident TGFbeta-related proteins in neuronal patterning in the dorsal spinal cord. *Cell* **91**, 127-138.
Lupo, G., Novorol, C., Smith, J. R., Vallier, L., Miranda, E., Alexander, M., Biagioni, S., Pedersen, R. A. and Harris, W. A. (2013). Multiple roles of Activin/Nodal, bone morphogenetic protein, fibroblast growth factor and Wnt/beta-catenin signalling in the anterior neural patterning of adherent human embryonic stem cell cultures. *Open Biol.* **3**, 120167.
Lustig, B., Jerchow, B., Sachs, M., Weiler, S., Pietsch, T., Karsten, U., van de Wetering, M., Clevers, H., Schlag, P. M., Birchmeier, W. et al. (2002). Negative feedback loop of Wnt signaling through upregulation of conductin/axin2 in colorectal and liver tumors. *Mol. Cell. Biol.* **22**, 1184-1193.
Mayor, R., Guerrero, N. and Martinez, C. (1997). Role of FGF and noggin in neural crest induction. *Dev. Biol.* **189**, 1-12.
Menendez, L., Yatskievych, T. A., Antin, P. B. and Dalton, S. (2011). Wnt signaling and a Smad pathway blockade direct the differentiation of human pluripotent stem cells to multipotent neural crest cells. *Proc. Natl. Acad. Sci. USA* **108**, 19240-19245.
Mica, Y., Lee, G., Chambers, S. M., Tomishima, M. J. and Studer, L. (2013). Modeling neural crest induction, melanocyte specification, and disease-related pigmentation defects in hESCs and patient-specific iPSCs. *Cell Rep.* **3**, 1140-1152.
Miyoshi, T., Maruhashi, M., Van De Putte, T., Kondoh, H., Huylebroeck, D. and Higashi, Y. (2006). Complementary expression pattern of Zfhx1 genes Sip1 and deltaEF1 in the mouse embryo and their genetic interaction revealed by compound mutants. *Dev. Dyn.* **235**, 1941-1952.
Nakanishi, M., Kurisaki, A., Hayashi, Y., Warashina, M., Ishiura, S., Kusuda-Furue, M. and Asashima, M. (2009). Directed induction of anterior and posterior primitive streak by Wnt from embryonic stem cells cultured in a chemically defined serum-free medium. *FASEB J.* **23**, 114-122.
Nakata, K., Nagai, T., Aruga, J. and Mikoshiba, K. (1997). Xenopus Zic3, a primary regulator both in neural and neural crest development. *Proc. Natl. Acad. Sci. USA* **94**, 11980-11985.
Park, D.-S., Seo, J.-H., Hong, M., Bang, W., Han, J.-K. and Choi, S.-C. (2013). Role of Sp5 as an essential early regulator of neural crest specification in xenopus. *Dev. Dyn.* **242**, 1382-1394.
Patthey, C. and Gunhaga, L. (2014). Signaling pathways regulating ectodermal cell fate choices. *Exp. Cell Res.* **321**, 11-16.
Patthey, C., Edlund, T. and Gunhaga, L. (2009). Wnt-regulated temporal control of BMP exposure directs the choice between neural plate border and epidermal fate. *Development* **136**, 73-83.
Pera, M. F. and Trounson, A. O. (2004). Human embryonic stem cells: prospects for development. *Development* **131**, 5515-5525.
Pera, M. F., Andrade, J., Houssami, S., Reubinoff, B., Trounson, A., Stanley, E. G., Ward-van Oostwaard, D. and Mummery, C. (2004). Regulation of human embryonic stem cell differentiation by BMP-2 and its antagonist noggin. *J. Cell Sci.* **117**, 1269-1280.
Phillips, B. T., Kwon, H.-J., Melton, C., Houghtaling, P., Fritz, A. and Riley, B. B. (2006). Zebrafish msxB, msxC and msxE function together to refine the neural-nonneural border and regulate cranial placodes and neural crest development. *Dev. Biol.* **294**, 376-390.

Pieper, M., Ahrens, K., Rink, E., Peter, A. and Schlosser, G. (2012). Differential distribution of competence for panplacodal and neural crest induction to non-neural and neural ectoderm. *Development* **139**, 1175-1187.
Rodda, S. J., Kavanagh, S. J., Rathjen, J. and Rathjen, P. D. (2002). Embryonic stem cell differentiation and the analysis of mammalian development. *Int. J. Dev. Biol.* **46**, 449-458.
Sasai, Y. (2013). Next-generation regenerative medicine: organogenesis from stem cells in 3D culture. *Cell Stem Cell* **12**, 520-530.
Sato, T., Sasai, N. and Sasai, Y. (2005). Neural crest determination by co-activation of Pax3 and Zic1 genes in Xenopus ectoderm. *Development* **132**, 2355-2363.
Savage, R. and Phillips, C. R. (1989). Signals from the dorsal blastopore lip region during gastrulation bias the ectoderm toward a nonepidermal pathway of differentiation in Xenopus laevis. *Dev. Biol.* **133**, 157-168.
Schlosser, G. (2008). Do vertebrate neural crest and cranial placodes have a common evolutionary origin?. *Bioessays* **30**, 659-672.
Selleck, M. A. and Bronner-Fraser, M. (1995). Origins of the avian neural crest: the role of neural plate-epidermal interactions. *Development* **121**, 525-538.
Shelton, M., Metz, J., Liu, J., Carpenedo, R. L., Demers, S.-P., Stanford, W. L. and Skerjanc, I. S. (2014). Derivation and expansion of PAX7-positive muscle progenitors from human and mouse embryonic stem cells. *Stem Cell Rep.* **3**, 516-529.
Smith, J. R., Vallier, L., Lupo, G., Alexander, M., Harris, W. A. and Pedersen, R. A. (2008). Inhibition of Activin/Nodal signaling promotes specification of human embryonic stem cells into neuroectoderm. *Dev. Biol.* **313**, 107-117.
Spagnoli, F. M. and Hemmati-Brivanlou, A. (2006). Guiding embryonic stem cells towards differentiation: lessons from molecular embryology. *Curr. Opin. Genet. Dev.* **16**, 469-475.
Stewart, S. A., Dykxhoorn, D. M., Palliser, D., Mizuno, H., Yu, E. Y., An, D. S., Sabatini, D. M., Chen, I. S. Y., Hahn, W. C., Sharp, P. A. et al. (2003). Lentivirus-delivered stable gene silencing by RNAi in primary cells. *RNA* **9**, 493-501.
Streit, A. and Stern, C. D. (1999). Establishment and maintenance of the border of the neural plate in the chick: involvement of FGF and BMP activity. *Mech. Dev.* **82**, 51-66.
Streit, A., Berliner, A. J., Papanayotou, C., Sirulnik, A. and Stern, C. D. (2000). Initiation of neural induction by FGF signalling before gastrulation. *Nature* **406**, 74-78.
Stuhlmiller, T. J. and Garcia-Castro, M. I. (2012a). Current perspectives of the signaling pathways directing neural crest induction. *Cell. Mol. Life Sci.* **69**, 3715-3737.
Stuhlmiller, T. J. and Garcia-Castro, M. I. (2012b). FGF/MAPK signaling is required in the gastrula epiblast for avian neural crest induction. *Development* **139**, 289-300.
Sumi, T., Tsuneyoshi, N., Nakatsuji, N. and Suemori, H. (2008). Defining early lineage specification of human embryonic stem cells by the orchestrated balance of canonical Wnt/beta-catenin, Activin/Nodal and BMP signaling. *Development* **135**, 2969-2979.
Surmacz, B., Fox, H., Gutteridge, A., Fish, P., Lubitz, S. and Whiting, P. (2012). Directing differentiation of human embryonic stem cells toward anterior neural ectoderm using small molecules. *Stem Cells* **30**, 1875-1884.
Tan, J. Y., Sriram, G., Rufaihah, A. J., Neoh, K. G. and Cao, T. (2013). Efficient derivation of lateral plate and paraxial mesoderm subtypes from human embryonic stem cells through GSKi-mediated differentiation. *Stem Cells Dev.* **22**, 1893-1906.
Tribulo, C., Aybar, M. J., Nguyen, V. H., Mullins, M. C. and Mayor, R. (2003). Regulation of Msx genes by a Bmp gradient is essential for neural crest specification. *Development* **130**, 6441-6452.
Tsakiridis, A., Huang, Y., Blin, G., Skylaki, S., Wymeersch, F., Osorno, R., Economou, C., Karagianni, E., Zhao, S., Lowell, S. et al. (2015). Distinct Wnt-driven primitive streak-like populations reflect in vivo lineage precursors. *Development* **142**, 809.
Umeda, K., Zhao, J., Simmons, P., Stanley, E., Elefanty, A. and Nakayama, N. (2012). Human chondrogenic paraxial mesoderm, directed specification and prospective isolation from pluripotent stem cells. *Sci. Rep.* **2**, 455.
Umeda, K., Oda, H., Yan, Q., Matthias, N., Zhao, J., Davis, B. R. and Nakayama, N. (2015). Long-term expandable SOX9(+) chondrogenic ectomesenchymal cells from human pluripotent stem cells. *Stem Cell Rep.* **4**, 712-726.
Vallier, L., Touboul, T., Chng, Z., Brimpari, M., Hannan, N., Millan, E., Smithers, L. E., Trotter, M., Rugg-Gunn, P., Weber, A. et al. (2009). Early cell fate decisions of human embryonic stem cells and mouse epiblast stem cells are controlled by the same signalling pathways. *PLoS ONE* **4**, e6082.
Van de Putte, T., Maruhashi, M., Francis, A., Nelles, L., Kondoh, H., Huylebroeck, D. and Higashi, Y. (2003). Mice lacking ZFHX1B, the gene that codes for Smad-interacting protein-1, reveal a role for multiple neural crest cell defects in the etiology of Hirschsprung disease-mental retardation syndrome. *Am. J. Hum. Genet.* **72**, 465-470.
Wakamatsu, N., Yamada, Y., Yamada, K., Ono, T., Nomura, N., Taniguchi, H., Kitoh, H., Mutoh, N., Yamanaka, T., Mushiake, K. et al. (2001). Mutations in SIP1, encoding Smad interacting protein-1, cause a form of Hirschsprung disease. *Nat. Genet.* **27**, 369-370.
Wilson, S. I., Graziano, E., Harland, R., Jessell, T. M. and Edlund, T. (2000). An early requirement for FGF signalling in the acquisition of neural cell fate in the chick embryo. *Curr. Biol.* **10**, 421-429.
Wilson, S., Rydstrom, A., Trimborn, T., Willert, K., Nusse, R., Jessell, T. M. and Edlund, T. (2001). The status of Wnt signalling regulates neural and epidermal fates in the chick embryo. *Nature* **411**, 325-330.
Yardley, N. and Garcia-Castro, M. I. (2012). FGF signaling transforms non-neural ectoderm into neural crest. *Dev. Biol.* **372**, 166-177.
Zhang, J. and Jacobson, A. G. (1993). Evidence that the border of the neural plate may be positioned by the interaction between signals that induce ventral and dorsal mesoderm. *Dev. Dyn.* **196**, 79-90.
Zhang, X., Huang, C. T., Chen, J., Pankratz, M. T., Xi, J., Li, J., Yang, Y., LaVaute, T. M., Li, X.-J., Ayala, M. et al. (2010). Pax6 is a human neuroectoderm cell fate determinant. *Cell Stem Cell* **7**, 90-100.
zur Nieden, N. I., Kempka, G. and Ahr, H. J. (2003). In vitro differentiation of embryonic stem cells into mineralized osteoblasts. *Differentiation* **71**, 18-27.

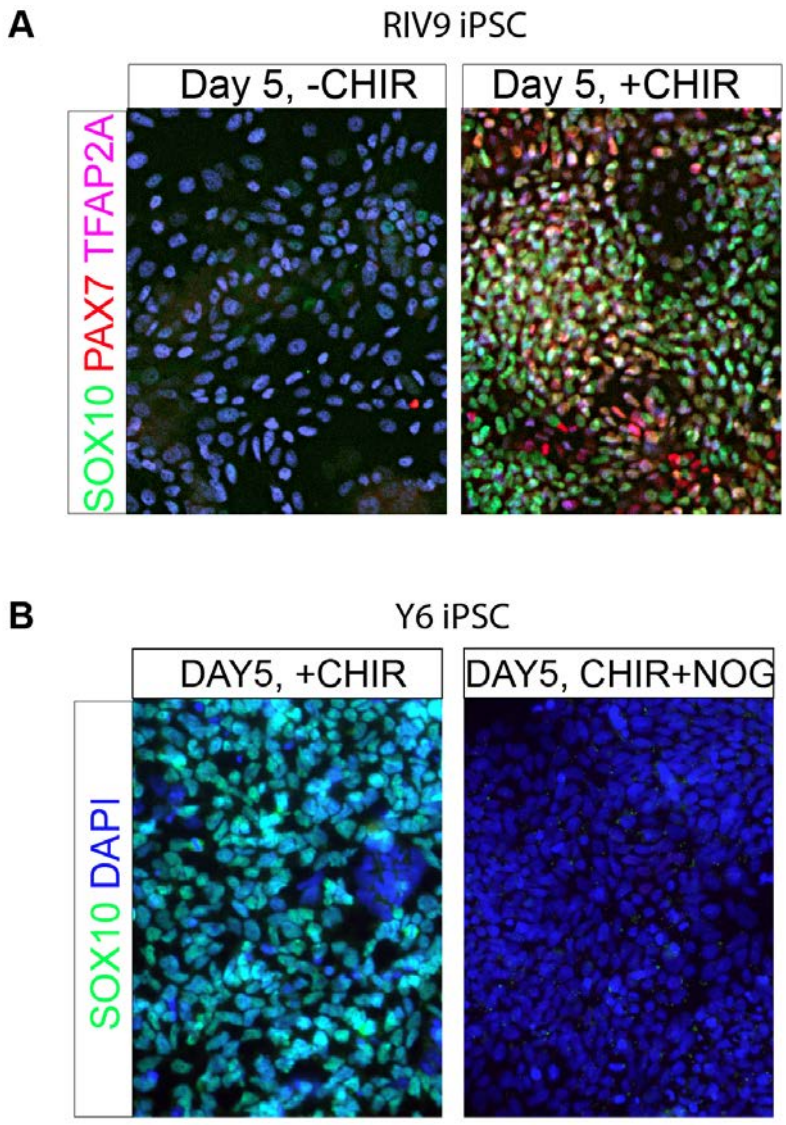

Supplementary figure 1. CHIR 99021 induces neural crest cells in human Y6 iPSCs. SOX10 (green), PAX7 (red) and TFAP2 (violet) triple immunostaining of iPSC RIV9 cultured after dissociation under control (No CHIR) or with CHIR for 5 days. SOX10 staining of day 5 Y6 iPSC cultures treated continuously with 3 μM CHIR and with or without 300 ng/mL NOGGIN from day 0 to day 1.

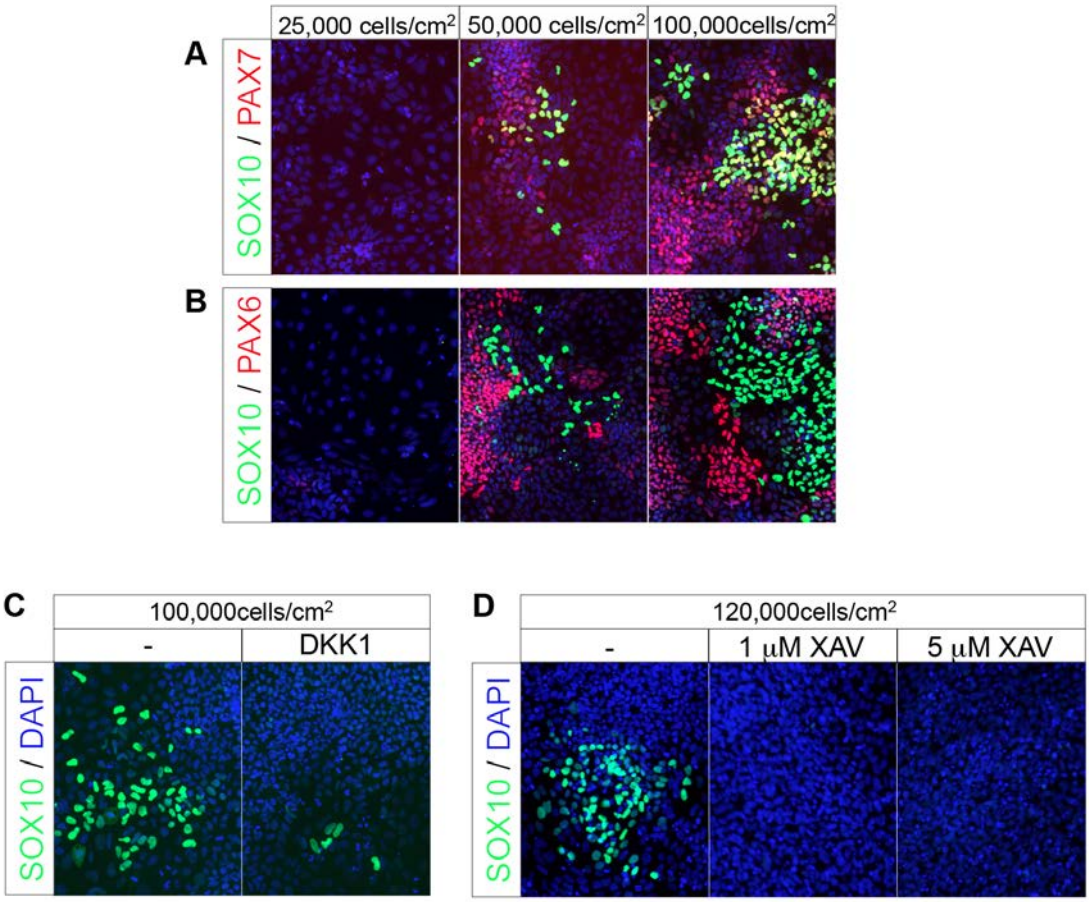

Supplementary figure 2. Spontaneous induction of SOX10$^+$, PAX7$^+$ and PAX6$^+$ cells in high-density cultures. A, B. Dissociated hESCs were plated at the indicated densities and cultured for 5 days in the base medium for NC induction without the administration of CHIR. SOX10/PAX7 (A) and SOX10/PAX6 (B) double labeling were performed. C. Day 5 cultures at the indicated initial seeding density were treated with or without 100 ng/mL DKK1 for 5 days and were stained with SOX10 antibody. D. Differentiating hESCs cultured in base differentiation medium without CHIR were treated with or without XAV 939 (XAV) at the indicated concentrations. Day 5 cultures were collected for SOX10 immunofluorescence.

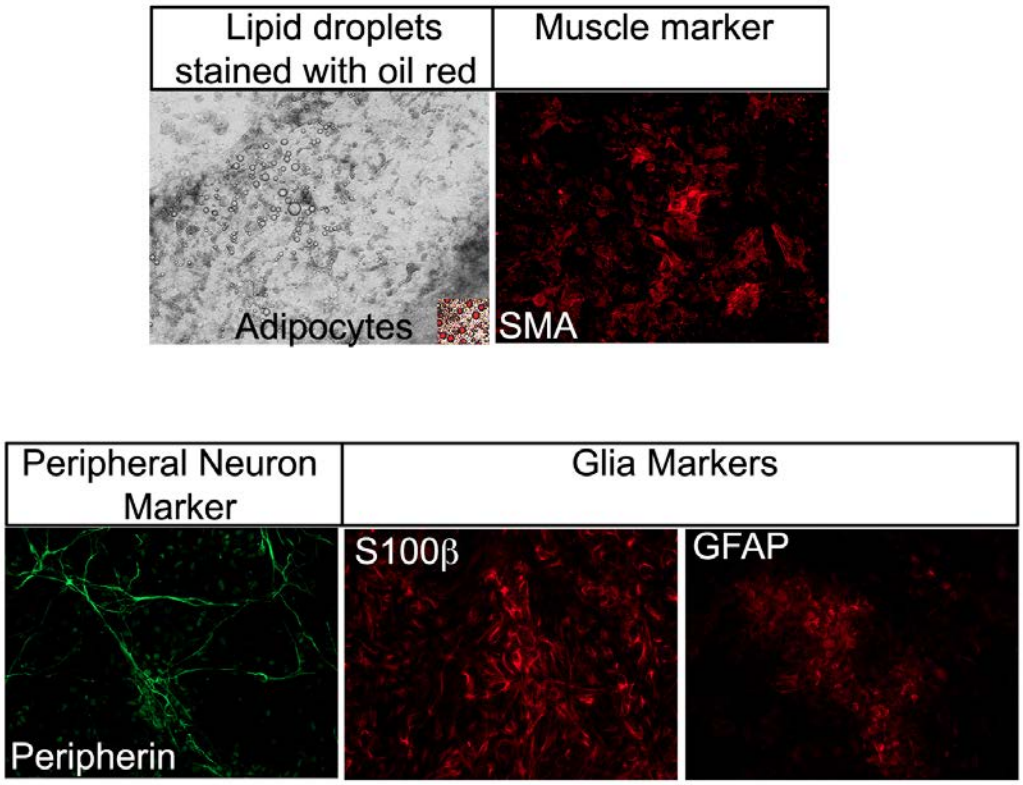

Supplementary figure 3. Terminal neural crest derivatives derived from WNT3a induced neural crest cells. Dissociated hESCs were induced for 5 days in Wnt3a (10 ng/ml) prior to being assayed for their ability to produce neural crest derivatives. Assays were specific to the derivatives of interest.

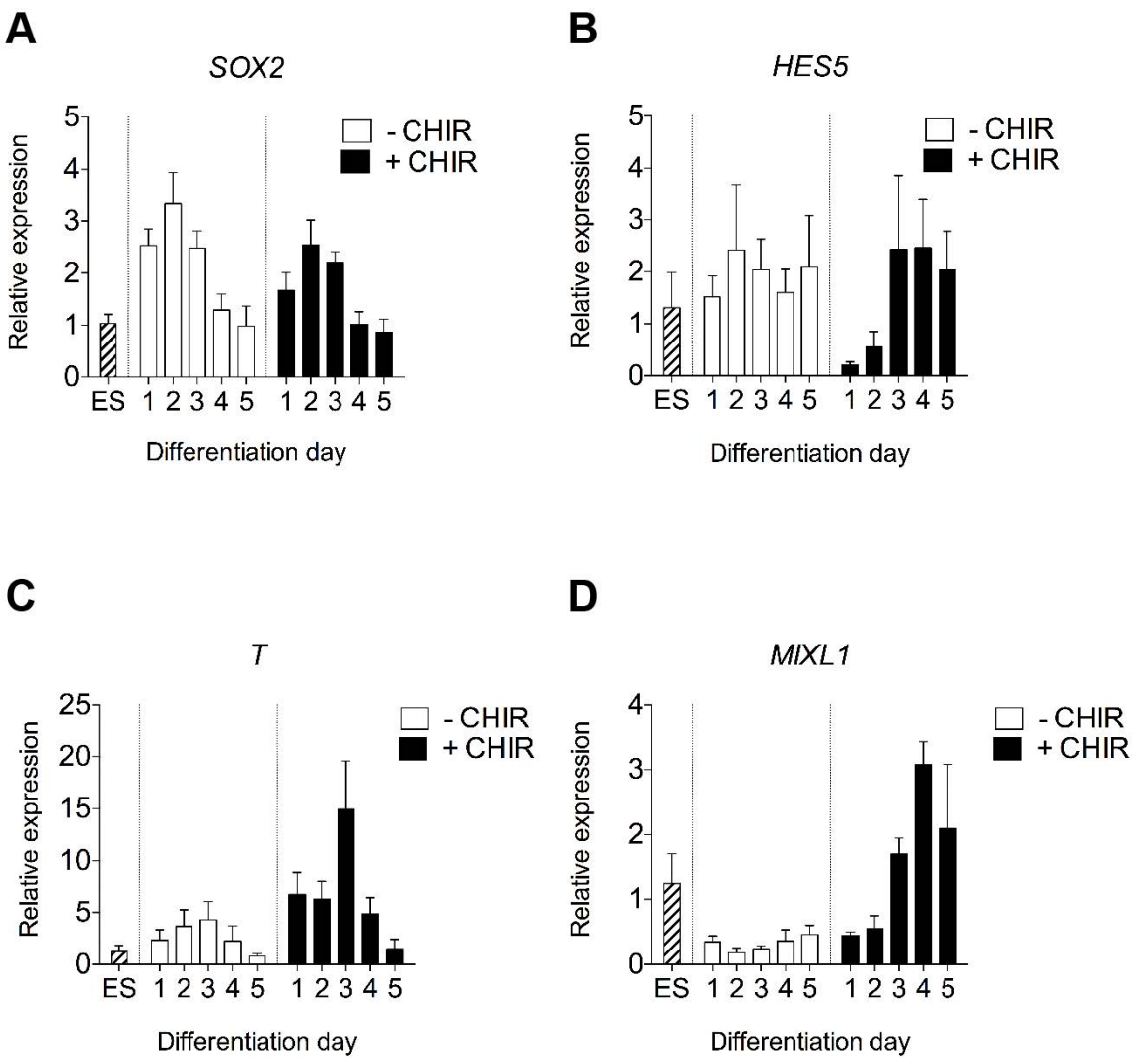

Supplementary figure 4. Expression of neural and mesoderm associated transcripts during human NC induction. A-D. Time course real time PCR assays of *SOX2*, *HES5*, *T* and *MIXL1* during human NC induction.

Supplementary table 1. Human primer sequences for real-time PCR of gene markers during ESC differentiation.

Transcript	Forward	Reverse
ACTB	TGAACCCCAAGGCCAACCGC	GACCCCGTCACCGGAGTCCA
AXIN2	AGTCAGCAGAGGGACAGGAA	AGCTCTGAGCCTTCAGCATC
CHD1/E-CADHERIN	GGATGTGCTGGATGTGAATG	CTCAAAATCCTCCCTGTCCA
CTNNB1	TCCCACTGGCCTCTGATAAA	AACTAGTCGTGGAATGGCAC
ΔNp63	GGAAAACAATGCCCAGACTC	GTGGAATACGTCCAGGTGGC
DLX5	ACGCTAGCTCCTACCACCAG	TTTGCCATTCACCATTCTCA
FOXD3	GCATCTGCGAGTTCATCAGC	CGTTGAGTGAGAGGTTGTGG
GATA3	GAGGAGGTGGATGTGCTTTT	CAGGGTAGGGATCCATGAAG
HES5	CTCAGCCCCAAAGAGAAAAA	TAGTCCTGGTGCAGGCTCTT
MIXL1	AGCTGCTGGAGCTCGTCTTC	TGGAAGGATTTCCCACTCTG
MSX1	CTGCACCCTCCGCAAACACA	AGGCTGAGCGAGCTGGAGAA
MSX2	CGGTCAAGTCGGAAAATTCA	GAGGAGCTGGGATGTGGTAA
NANOG	CAAAGGCAAACAACCCACTT	TCTGCTGGAGGCTGAGGTAT
NR2F1	CGAGTACAGCTGCCTCAAAG	TACTGGCTCCTCACGTACTC
OCT4	GAAGGATGTGGTCCGAGTGT	GTGAAGTGAGGGCTCCCATA
PAX3	AATTACTCAAGGACGCGGTC	TTCTTCTCGCTTTCCTCTGC
PAX6	CACCTACAGCGCTCTGCCGC	CCCGAGGTGCCCATTGGCTG
PAX7	TGACAGCTTCATGAATCCGG	GATGGAGAAGTCAGCCTGTG
SIX1	TCAGCTCCAAGACTCTCTGC	ACAAGCTGCAAAAATGTTCC
SNAI2	CAGACCCTGGTTGCTTCAAG	GAGCCCTCAGATTTGACCTG
SOX2	TCAAGCGGCCCATGAATGCC	AGCCGCTTAGCCTCGTCGAT
SOX10	CTCTGGAGGCTGCTGAA	TGGGCTGGTACTTGTAGTC
T	AGGCTCCCGTCTCCTTCAGCAA	TGGCTGGTGATCATGCGCTGT
TFAP2A	GATCCTCGCAGGGACTACAG	TACCCGGGTCTTCTACATGC
ZIC1	GTCCTACACGCATCCCAGTT	GCGATAAGGAGCTTGTGGTC
ZIC3	AAGTCTTTCAAGGCGAAGTA	GTCACAGCCTTCAAATTCAC

Supplementary table 2. Short-hairpin RNA sequences and information for knockdown experiments in hESCs.

Transcripts	ID	RNA consortium Clone ID	Target sequence	Match region	Knockdown efficiency*
CTNNB1	shRNA1	TRCN0000003844	CGCATGGAAGAAATAGTTGAA	CDS	62%
CTNNB1	**shRNA2**	**TRCN0000314921**	**TCTAACCTCACTTGCAATAAT**	**CDS**	**82%**
CTNNB1	shRNA3	TRCN0000010824	CCATTGTTTGTGCAGCTGCTT	CDS	46%
PAX6	shRNA1	TRCN0000016123	GCAAGAATACAGGTATGGTTT	CDS	74%
PAX6	shRNA2	TRCN0000016125	CGTCCATCTTTGCTTGGGAAA	CDS	68%
PAX6	**shRNA3**	**TRCN0000246162**	**ATACGCACTGTTGGTACAATT**	**3UTR**	**97%**

*Knockdown efficiency was measured by real-time PCR in undifferentiated hESCs and differentiated ESC cultures at day 5 for *CTNNB1* and *PAX6* respectively. The species with the highest knockdown were bolded and selected for functional analyses.

Supplementary table 3. Antibodies used for immunofluorescence.

Protein/Gene	Source	Catalog no.	Antibody type	Dilution
PAX7	Developmental hybridoma bank	Pax7	Mouse IgG1	1:50
PAX6	Developmental hybridoma bank	Pax6	Mouse IgG1	1:100
TFAP2A	Developmental hybridoma bank	3B5	Mouse IgG2b	1:50
ISL1	Developmental hybridoma bank	Isl1/2	Mouse IgG2b	1:100
SOX10	Vivian Lee	-	Rabbit	1:3000
POU5F1 (OCT4)	Santa Cruz Biotechnology	SC-5279	Mouse IgG2b	1:250
T (BRACHYURY)	R&D Systems	AF2085	Goat	1:200
HuC/D	Molecular probe	A-21271	Mouse IgG2b	1:300
S100β	Thermo-Scientific	MA1-2505	Mouse IgG1	1:100
MITF	R&D Systems	AF5769	Goat	1:50
PRPH	Millipore	AB1530	Rabbit	1:200
TUJ1	Covance	MMS-435P-250	Mouse IgG2a	1:2000
GFAP	Covance	SMI-22R	mouse IgG2b	1:500